*The Annals of Applied Probability*
2015, Vol. 25, No. 3, 1232–1278
DOI: 10.1214/14-AAP1021


# ASYMPTOTIC DOMINO STATISTICS IN THE AZTEC DIAMOND

BY SUNIL CHHITA[1], KURT JOHANSSON[1,2] AND BENJAMIN YOUNG[1]

*University of Bonn, Royal Institute of Technology (KTH) and University of Oregon*

We study random domino tilings of the Aztec diamond with different weights for horizontal and vertical dominoes. A domino tiling of an Aztec diamond can also be described by a particle system which is a determinantal process. We give a relation between the correlation kernel for this process and the inverse Kasteleyn matrix of the Aztec diamond. This gives a formula for the inverse Kasteleyn matrix which generalizes a result of Helfgott. As an application, we investigate the asymptotics of the process formed by the southern dominoes close to the frozen boundary. We find that at the northern boundary, the southern domino process converges to a thinned Airy point process. At the southern boundary, the process of holes of the southern domino process converges to a multiple point process that we call the thickened Airy point process. We also study the convergence of the domino process in the unfrozen region to the limiting Gibbs measure.

**1. Introduction.** The *Aztec Diamond of order n* is a planar region which can be completely tiled with *dominoes*, two-by-one rectangles. Over the past twenty years, this particular shape has come to occupy a central place in the literature of domino tilings of plane regions. Tilings of large Aztec diamonds exhibit striking features—the main one being that these tilings exhibit a limit shape, described by the so-called Arctic circle theorem [20]. See Figure 1 for pictures of tilings of a relatively large Aztec diamond.

There are several alternate descriptions of a tiling of an Aztec diamond. A domino tiling is equivalent to a perfect matching, or *dimer cover*, on the dual graph of the region which is tiled. There is an equivalent family of nonintersecting lattice paths, called DR paths [36], and there is a description as a stack of a certain sort of blocks, called *Levitov blocks* [34, 35]; see Figure 1. There is also a well-studied *interlacing particle process* which is equivalent to the tiling model in a certain sense, but this equivalence is not bijective: there are $2^{n(n+1)/2}$ tilings of the Aztec diamond, whereas the number of configurations of the particle process are equinumerous with order-$n$ *alternating sign matrices* or configurations of the

Received January 2013; revised January 2014.
[1]Supported by the Knut and Alice Wallenberg Foundation Grant KAW:2010.0063.
[2]Supported by the Swedish Research Council (VR).
*MSC2010 subject classifications.* Primary 60G55; secondary 60C05.
*Key words and phrases.* Aztec diamond, domino tiling, dimer covering, determinantal point process.

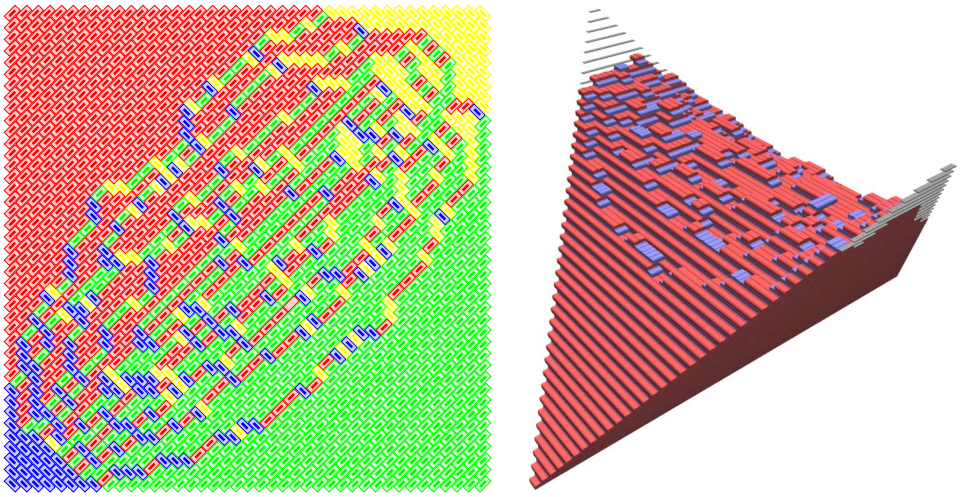

FIG. 1. *Left*: *a tiling of an Aztec diamond of order* 41 *with* $a = \frac{1}{2}$, *and the corresponding dimer cover. The green dominoes along each horizontal row give the southern domino process. Right*: *the height function associated to this tiling* (*realized as a pile of Levitov blocks* [34, 35]).

*six-vertex model*. However, the correspondence is *weight preserving* and *locally defined*; it maps certain collection of tilings to a configuration of the *free-fermion* six-vertex model [15], preserving the relative weights.

It is this point process whose local asymptotics have been studied most thoroughly [22]; in particular, the boundary of the frozen region is more easily described using the particles, since it is related to the position of the last particles on different lines. There is also a relationship between these particles and a certain sort of *zig-zag path* in the tiling (distinct from the zig-zag paths studied in [7]) which is helpful. However, the many-to-one nature of the correspondence necessarily loses some of the information about the original tilings. In both the domino and particle pictures, we get determinantal point processes, although the precise combinatorial relation between the two processes is not immediate.

We correct this situation in this paper, by giving a formula for the inverse Kasteleyn matrix for the Aztec diamond. This generalizes a previous result by Helfgott [19] to the case when the horizontal and vertical dominoes have different weights. Using an observation of Kenyon [29], it is then possible to compute probabilities for various configurations of dominoes and their asymptotic limits as the size of the Aztec diamond increases. In particular, we find the behavior of the boundary of the frozen region when we can only see one type of domino.

1.1. *The southern domino process*: *North boundary.* There are in fact four different types of dominoes in a tiling: the dominoes can be placed in two orientations, each of which comes in two different parities (determined by the bipartition

of the dual graph on which the dominoes are placed). Due to the Arctic circle theorem, with probability one, there are only dominoes of one of these four types clustered near each of the four corners of the Aztec diamond. For this reason (and others, see [15]) we call the four types of dominoes *north*, *south*, *east and west*, which are colored red, green, yellow and blue in Figure 1 in the electronic version of this article.

For the moment, ignore all but the southern dominoes (the green ones in Figure 1). Viewing each domino as a *point*, the set of all southern dominoes form a determinantal point process. Note that the positions of the southern dominoes do not specify the tiling uniquely so they only give a partial description of the tiling (though, together with any of the other types of dominoes, they do). We analyze the distribution of the southern dominoes along a diagonal line in a large Aztec diamond, scaled so as to study the two intersections between this line and the frozen boundary of the tiling (an "arctic ellipse," in the weighted case). It would be possible to extend what we have done to analyze the joint distribution of all southern dominoes in the Aztec diamond; as is, our analysis extends previous results in [8] on placement probabilities of single dominoes.

We will show that the appropriate scaling limit of the point process of southern dominoes along a diagonal line close to the boundary of the *northern* frozen region is given by a thinned Airy kernel point process, where the amount of thinning depends on the relative weight of the horizontal and vertical dominoes. This can be heuristically understood in the following way. The Airy kernel point process, as mentioned earlier, is the edge limit of the particle process along a diagonal line, and these in turn are given by the intersections of the nonintersecting paths and the diagonal line. Sometimes these intersections occur along a southern domino, and sometimes not. If we only see the southern dominoes we only see some of these intersections, and which of them we see is essentially random; so we might expect, in the limit, a random thinning of the Airy kernel point process. A priori it is not clear that the thinning becomes independent in the limit, but this turns out to be the case.

1.2. *The southern domino process*: *Southern boundary.* If, instead, we examine the southern frozen region, we find that almost all of the dominoes are coming from the southern domino process and thus lie in a frozen, brickwork pattern predominantly. The southern boundary is a "hole" in this regular pattern. Consider the holes between the southern dominoes along a diagonal line in a neighborhood of the southern boundary. These holes also form a determinantal point process, but in a scaling limit it does not converge to a *simple* point process, but rather to a *multiple point process* with independent geometric probabilities for the multiple points in an Airy kernel point process. This can be seen in Figure 1: there is a tendency for dominoes of like types to cluster together along the southern boundary. This tendency continues even in the limit, with a cluster of $k$ dominoes becoming a point of multiplicity $k$. The multiplicity increases as we go toward the lower tangency point of the arctic ellipse, a fact which can also be observed in Figure 1.

1.3. *Previous work on domino tilings*. Domino tilings on the Aztec diamond were originally introduced in [15, 16] as a model connected with the *alternating sign matrices*. In this section, we give only a partial overview of the literature on the asymptotics of domino tilings of the Aztec diamond.

The limit shape for random tilings of the Aztec diamond, the so-called Arctic circle theorem, was first computed for $a = 1$ in [20], where $a$ is the weight of each vertical domino. Since then, there have been a variety of different and interesting approaches to compute the limit shape which hold for general $a$ [8, 22, 32, 40]. The existence of limit shapes is not limited to domino tilings; limit shapes also exist for random lozenge tilings, for example, the boxed plane partition [10]. These examples provided a motivation for a theory of the existence of limit shapes for general tiling models on bipartite graphs [9, 32].

The edge behavior, that is, the behavior between the frozen and unfrozen regions has, been of particular interest to the random matrix community, as the fluctuations are of size $n^{1/3}$. This is the same size as the fluctuations of the largest eigenvalue of the *Gaussian unitary ensemble* (*GUE*). Indeed, [21, 22] showed that the law of the particles associated to the tiling is given by the *Airy process* and that the position of the last particle is given by the Tracy Widom distribution, $F_2$; see, for example, [1]. Furthermore, Johansson and Nordenstam [24] showed that the distribution of these particles becomes the *GUE minor process* at the intersection of the liquid region and the boundary of the Aztec diamond while Fleming and Forrester [17] obtained similar results for a certain half Aztec diamond.

There are a handful of other explicitly inverted Kasteleyn matrices in the literature for domino tilings. The inverse of the Kasteleyn matrix of the Aztec diamond was computed by Helfgott [19] in the case of the uniform measure on domino tilings; the results in [9, 33] rely on explicit inverses of four Kasteleyn-like matrices that, together, count perfect matchings on a torus-embedded graph. Finally, Kasteleyn [25] and independently Temperley and Fisher in [42] compute the eigenvalues and eigenvectors of the Kasteleyn matrix of the $m \times n$ grid graph explicitly.

A proof of convergence to the Gaussian Free Field, following [3] should be possible. In fact, an earlier preprint of this paper (dated December 21, 2012 and posted on the arXiv) stated such a claim as Theorem 2.9 and outlined a proof, skipping over many details. We would like to retract this theorem and its outlined proof, for the following reason: the details that we omitted (largely estimates on $K^{-1}$) were numerous enough and technical enough that even a rather dedicated reader would have been hard-pressed to supply them all. Moreover, in revision, we found it impossible to include enough details of these estimates while keeping the discussion brief. The proof, if and when it appears in the literature, will have to be in its own paper. Instead, we include in Section 6 only a list of the estimates that would be needed in order to demonstrate convergence. We sincerely thank the anonymous referee for bringing this error to our attention.

**2. Results.** In this section, we give the results of our paper and the necessary prerequisites to understand these results. There are three types of results:

(1) the inverse of the Kasteleyn matrix (Section 2.1),
(2) results on the southern domino process close to the edges of the unfrozen region (Section 2.2),
(3) local Gibbs measure (Section 2.3).

2.1. *The inverse of the Kasteleyn matrix.*

2.1.1. *Definitions.* In this paper, the Aztec diamond is rotated by $\pi/4$ counter clockwise from the convention set in [15]. Because there are many possibilities for coordinate systems of Aztec diamonds, we will refer to our coordinate system as the *Kasteleyn coordinates*. In the Kasteleyn coordinates, an *Aztec diamond of order* $n$ consists of squares with corners $(k-1,l)$, $(k,l-1)$, $(k+1,l)$ and $(k,l+1)$ for either $k \bmod 2 = 1$ and $l \bmod 2 = 0$ with $1 \le k \le 2n-1$ and $0 \le l \le 2n$, or $k \bmod 2 = 0$ and $l \bmod 2 = 1$ with $0 \le k \le 2n$ and $1 \le l \le 2n-1$. A *domino* is a union of two adjacent squares which share an edge. A *domino tiling* of the Aztec diamond is any arrangement of dominoes such that each square of the Aztec diamond is covered exactly once by a domino.

The dual graph of the Aztec diamond (without its external face) is a bipartite graph which has vertices $\mathtt{W} \cup \mathtt{B}$ where

$$\mathtt{W} = \{(x_1,x_2) : x_1 \bmod 2 = 1, x_2 \bmod 2 = 0, \\ 1 \le x_1 \le 2n-1, 0 \le x_2 \le 2n\} \tag{2.1}$$

and

$$\mathtt{B} = \{(x_1,x_2) : x_1 \bmod 2 = 0, x_2 \bmod 2 = 1, \\ 0 \le x_1 \le 2n, 1 \le x_2 \le 2n-1\}, \tag{2.2}$$

which correspond to the white and black vertices, respectively, written in terms of the Kasteleyn coordinates. To distinguish between the primal and dual graphs, we will refer to the dual graph of the Aztec diamond as the *Aztec diamond graph*. We shall also set $e_1 = (1,1)$ and $e_2 = (-1,1)$. The edge set of the Aztec diamond graph consists of all the edges $(x,y)$ with $y - x \pm e_i$ for $i \in \{1,2\}$ for $x \in \mathtt{W}$ and $y \in \mathtt{B}$.

A domino on the dual graph is an edge which is called a *dimer*. A domino tiling on the dual graph is a subset of edges such that each vertex is incident to exactly one edge. This collection of edges is called a *dimer covering*. Domino tilings of the Aztec diamond are equivalent to dimer coverings of the Aztec diamond graph. See Figure 2 for the Aztec diamond graph with its coordinates and an example of a dimer covering.

For $b \in \mathtt{B}$ and $w \in \mathtt{W}$, we say that a dimer $(b,w)$ is:

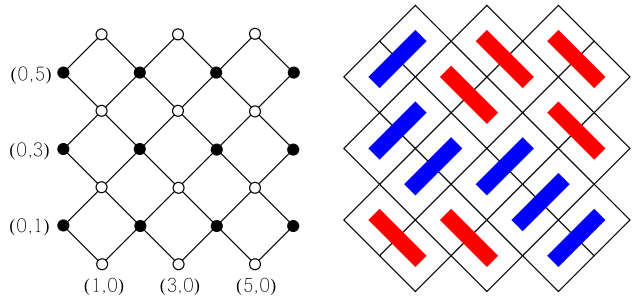


FIG. 2. *The figure on the right shows the coordinates of the Aztec diamond graph with the white and black vertices drawn in. The figure on the right shows an Aztec diamond of size* 3 *with a dimer covering of the dual graph. The domino tiling can be seen by placing dominoes over the dimers.*

- a *north* dimer if $w = b + e_1$,
- an *east* dimer if $w = b + e_2$,
- a *south* dimer if $w = b - e_1$,
- a *west* dimer if $w = b - e_2$.

There is a corresponding notion for dominoes, and this terminology agrees with that introduced in [20]. We will interchange between dominoes and dimers.

2.1.2. *Determinantal point processes.* Determinantal point processes are a key part of the analysis used in this paper. Here, we briefly describe these processes but more in-depth treatises of determinantal point processes can be found in [23] and [41].

Let $\Lambda$ be a Polish space, and take $\mathcal{M}(\Lambda)$ to denote the space of counting measures $\xi$ on $\Lambda$ with $\xi(B) < \infty$ for every bounded $B \subset \Lambda$. A point process on $\Lambda$ is a probability measure $\mathbb{P}$ on $\mathcal{M}(\Lambda)$. Let $M_n$ denote the factorial moment measure, that is, for disjoint Borel sets $A_1, \dots, A_m$ in $\Lambda$ and for all $(n_1, \dots, n_m) \in \mathbb{N}^m$

$$M_n\big(A_1^{n_1} \times \cdots \times A_m^{n_m}\big) = \mathbb{E}\left[\prod_{i=1}^{m} \frac{\xi(A_i)!}{(\xi(A_i) - n_i)!}\right]. \tag{2.3}$$

Suppose that $\lambda$ is a reference measure on $\Lambda$. For example, if $\Lambda = \mathbb{R}$, we can choose $\lambda$ to be the Lebesgue measure. If

$$M_n(A_1, \dots, A_n) = \int_{A_1 \times \cdots \times A_n} \rho_n(x_1, \dots, x_n)\, d\lambda(x_1) \cdots d\lambda(x_n) \tag{2.4}$$

for all Borel sets $A_i$ in $\Lambda$, we call $\rho_n$ to be the $n$th correlation function. For discrete processes, $\rho_n(x_1, \dots, x_n)$ is equal to the probability of $n$-tuples of particles at $x_1, \dots, x_n$, whereas for continuous processes, $\rho_n$ is the density of seeing particles. For example, if $\rho_n(x_1, \dots, x_n) = \rho(x_1) \cdots \rho(x_n)$ where $\rho \in L^1$ with $\Lambda = \mathbb{R}$ and $\lambda$ is the Lebesgue measure, then the point process is the Poisson point process on $\mathbb{R}$.

A point process is called *determinantal* if there exists a function $\mathbb{K}: \Lambda \times \Lambda \to \mathbb{C}$ called the correlation kernel, with

$$\rho_n(x_1, \dots, x_n) = \det\big(\mathbb{K}(x_i, x_j)\big)_{i,j=1}^{n}. \tag{2.5}$$

This leads to the following characterization of a determinantal point process. Let $C_c^+(\Lambda)$ be the set of all nonnegative continuous functions on $\Lambda$ with compact support. Take $\psi \in C_c^+(\Lambda)$, let $A$ denote the support of $\psi$ and set $\phi = 1 - e^{-\psi}$. Let $\mathbb{I}_A$ denote the indicator function for the set $A$. Then, provided $\phi\mathbb{K}\mathbb{I}_A$ is trace class, and the Fredholm determinant is given by its Fredholm expansion,

$$\mathbb{E}\big[e^{-\sum_j \psi(x_j)}\big] = \det(I - \phi\mathbb{K}\mathbb{I}_A)_{L^2(\Lambda,\lambda)}, \tag{2.6}$$

where $x_j$ are the points in the process.

2.1.3. *Particles.* Another way of viewing domino tilings of an Aztec diamond is a particle system formed from the zig-zag particles used in [22]. These particles can be described as follows: for $w \in \mathbb{W}$, we have a blue particle at $w$ if and only if a dimer covers the edge $(w + e_1, w)$ or the edge $(w - e_2, w)$. For $b \in \mathbb{B}$, we have a red particle at $b$ if and only if a dimer covers the edge $(b, b - e_1)$ or the edge $(b, b - e_2)$. By this setup, particles are present on south and west dimers, with blue particles sitting on white vertices and red particles sitting on black vertices.

The particle system considered in [22] came with its own coordinate system; see Figure 4 in Section 2 of that paper. The transformation between that system of coordinates and the Kasteleyn coordinates is

$$\begin{cases} u_1 = x_2, \\ u_2 = \dfrac{x_2 - x_1 + 1}{2}, \end{cases} \tag{2.7}$$

where $(u_1, u_2)$ are the particle coordinates and $(x_1, x_2)$ are the Kasteleyn coordinates. Figure 3 shows the red–blue particles along with the corresponding tiling.

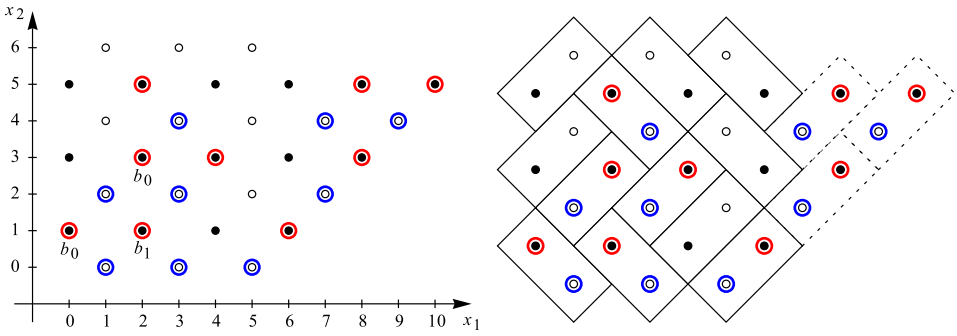


FIG. 3. *The figure on the left shows the red–blue particles with the Kasteleyn orientation for an Aztec diamond of size* 3 (*with additional vertices*). *The figure on the right shows the same configuration of red–blue particles with the domino tiling. This includes the three additional south dominoes.*

It is shown in [22] that the particles form a determinantal point process with correlation kernel given by

$$K_n(u_1,u_2;v_1,v_2)=\widetilde{K}_n(u_1,u_2;v_1,v_2)-\phi_{u_1,v_1}(u_2,v_2), \tag{2.8}$$

where

$$\begin{aligned}&\widetilde{K}_n(2r-\varepsilon_1,u_2;2s-\varepsilon_2,v_2)\\&\quad=\frac{1}{(2\pi i)^2}\int_{\gamma_{r_1}}\frac{dw}{w}\int_{\gamma_{r_2}}\frac{dz}{z}\frac{z^{v_2}}{w^{u_2}}\frac{(1-az)^{n-s+\varepsilon_2}(1+a/z)^s}{(1-aw)^{n-r+\varepsilon_1}(1+a/w)^r}\frac{w}{w-z},\end{aligned} \tag{2.9}$$

$$\begin{aligned}&\phi_{2r-\varepsilon_1,2s-\varepsilon_2}(u_2,v_2)\\&\quad=\frac{\mathbb{I}(2r-\varepsilon_1<2s-\varepsilon_2)}{2\pi i}\int_{\gamma_1}z^{v_2-u_2}\frac{(1-az)^{r-s+\varepsilon_2-\varepsilon_1}}{(1+a/z)^{r-s}}\frac{dz}{z}\end{aligned} \tag{2.10}$$

and $\varepsilon_1,\varepsilon_2\in\{0,1\}$, $a<r_1<1/a$, $0<r_2<r_1$ and $\gamma_t$ denotes a circle around 0 with radius $t$. Before setting $a=1$, one has to make an appropriate deformation of contours.

2.1.4. *The Kasteleyn matrix and Kenyon's formula.* The Kasteleyn matrix, introduced in [25, 26], can be used to count the number of weighted dimer coverings of a graph, and the inverse of the Kasteleyn matrix can be used to compute local statistics [27].

For a finite bipartite graph $G$, a *Kasteleyn matrix* is a signed weighted adjacency matrix of the graph with rows indexed by black vertices and columns indexed by white vertices; see [31] for details. The sign is chosen according to a *Kasteleyn orientation* of the graph. This means assigning a sign (possibly complex valued) to each edge weight so that the product of the edge weights around each face is negative.

For the Aztec diamond graph, we denote $K$ to be the matrix with $K:\mathtt{B}\times\mathtt{W}\to\mathbb{C}$ where $K(b,w)=K_{b,w}$ for $b=(x_1,x_2)\in\mathtt{B}$ and $w\in\mathtt{W}$ with

$$K(b,w)=\begin{cases}(-1)^{l+(x_1+x_2-1)/2}, & \text{if } w=b+(-1)^l e_1\in\mathtt{W},\\ (-1)^{l+(x_1+x_2-1)/2}ai, & \text{if } w=b-(-1)^l e_2\in\mathtt{W},\\ 0, & \text{otherwise.}\end{cases} \tag{2.11}$$

This matrix is a *Kasteleyn matrix* for the Aztec diamond graph. This matrix is a Kasteleyn matrix for the Aztec diamond graph; see Figure 4.

THEOREM 2.1 ([25]). *The number of weighted dimer coverings of the Aztec diamond graph is equal to* $|\det K|$.

In [27], Kenyon found that the dimers form a determinantal point process with the correlation kernel written in terms of the inverse of the Kasteleyn matrix (referred to as the *inverse Kasteleyn matrix*). Here, we state that result for the Kasteleyn matrix given in (2.11). Suppose that $E=\{e_i\}_{i=1}^n$ are a collection of distinct edges with $e_i=(b_i,w_i)$, where $b_i$ and $w_i$ denote black and white vertices.

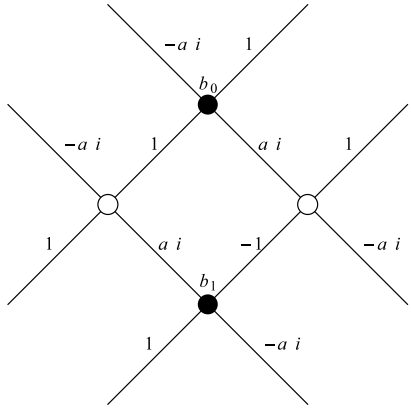


FIG. 4. *The complex weights associated to the Kasteleyn matrix given in* (2.11). *We have that the vertex* $b_i = (x_1, x_2)$ *has* $(x_1 + x_2 - 1)/2 \bmod 2 = i$ *for* $i \in \{0, 1\}$.

THEOREM 2.2. [27]. *The dimers form a determinantal point process on the edges of the Aztec diamond graph with correlation kernel given by*

$$L(e_i, e_j) = K(b_i, w_i) K^{-1}(w_j, b_i), \tag{2.12}$$

*where* $K(b, w) = K_{bw}$ *and* $K^{-1}(w, b) = (K^{-1})_{wb}$.

The above formula is sometimes referred to as *Kenyon's formula*.

PROOF OF THEOREM 2.2. By [27], we have that the probability of finding dimers at the edges $e_1, \dots, e_n$ is

$$\begin{aligned} \mathbb{P}(e_1, \dots, e_n) &= \prod_{i=1}^{n} K(b_i, w_i) \det\big(K^{-1}(w_j, b_i)\big)_{i,j=1}^{n} \\ &= \det\big(K(b_i, w_i) K^{-1}(w_j, b_i)\big)_{i,j=1}^{n} \\ &= \det\big(L(e_i, e_j)\big)_{i,j=1}^{n}. \end{aligned} \tag{2.13}$$

□

2.1.5. *The inverse Kasteleyn matrix.* The inverse Kasteleyn matrix for domino tilings of the Aztec diamond was originally computed in [19] for the case when $a = 1$. In that paper, Helfgott explicitly enumerated $K^{-1}(w, b) 2^{n(n+1)/2}$ which is the number of signed dimer coverings of an Aztec diamond graph with the vertices $w \in \mathtt{W}$ and $b \in \mathtt{B}$ removed. We generalize this formula so that we can consider different weights for vertical and horizontal tiles:

THEOREM 2.3. *For* $x = (x_1, x_2) \in \mathtt{W}$ *and* $y = (y_1, y_2) \in \mathtt{B}$, *we have*

$$K^{-1}(x, y) = \begin{cases} f_1(x, y), & \text{for } x_1 < y_1 + 1, \\ f_1(x, y) - f_2(x, y), & \text{for } x_1 \geq y_1 + 1, \end{cases} \tag{2.14}$$

*where*

$$f_1(x,y)=\frac{(-1)^{(y_1+y_2+x_1+x_2)/4}}{(2\pi i)^2}\times\int_{\mathcal{E}_2}\int_{\mathcal{E}_1}\frac{w^{y_1/2}}{z^{(x_1+1)/2}(w-z)}\times\frac{(a+z)^{x_2/2}(az-1)^{(2n-x_2)/2}}{(aw-1)^{(2n+1-y_2)/2}(a+w)^{(y_2+1)/2}}\,dz\,dw \tag{2.15}$$

*and*

$$f_2(x,y)=\frac{(-1)^{(x_1+x_2+y_1+y_2)/4}}{2\pi i}a^{(y_2-x_2-1)/2}\times\int_{\mathcal{E}_1}\frac{z^{(y_2-x_2-1)/2}(1/a+z)^{(y_1-x_1-1)/2}}{(1/a+a+z)^{(y_2-x_2+1)/2}}\,dz, \tag{2.16}$$

*where $\mathcal{E}_1$ is the positively oriented contour $|z|=\epsilon$, $\mathcal{E}_2$ is the positively oriented contour $|w-1/a|=\epsilon$ and the contours do not intersect.*

For domino tilings, the inverse Kasteleyn matrix cannot be obtained directly from the correlation kernel of the red–blue particles introduced in Section 2.1.3. However, the correlation kernel of the red–blue particles can be directly obtained from the inverse Kasteleyn matrix. This is different to lozenge tilings, where one can obtain the inverse Kasteleyn matrix from the interlaced particle system [4, 38].

We initially obtained the above expression for $K^{-1}$ using a guess based on Helfgott's formula in [19] for $K^{-1}$ when $a=1$, Theorem 2.2 and the correlation kernel for the particle system given in (2.8). In Section 3, we prove Theorem 2.3 by verifying the equation $K\cdot K^{-1}=\mathbb{I}$ for our conjectured formula for $K^{-1}$. In the proof, we expand $K\cdot K^{-1}$ entrywise, which gives a five-term relation involving entries of $K^{-1}$ due to the sparseness of the matrix $K$. A similar set of relations (without a boundary condition) was used in [5].

We can write the particle correlation kernel given in (2.8) in terms of the inverse Kasteleyn matrix. The relation is similar to that found in lozenge tiling; see [38] and [4]. Note that for lozenge tilings, the particle correlation kernel and the kernel from the inverse Kasteleyn matrix are in bijection. We find the following proposition.

PROPOSTION 2.4.

$$K^{-1}\big((x_1,x_2),(y_1,y_2)\big)=-(-1)^{(x_1-x_2+y_1-y_2)/4}K_n\left(y_2,\frac{y_2-y_1+1}{2};x_2,\frac{x_2-x_1+1}{2}\right). \tag{2.17}$$

We prove this proposition in Section 3.

2.2. *Edge fluctuations of southern dominoes.*

2.2.1. *Southern domino process.* From our expression for the inverse Kasteleyn matrix in Theorem 2.3 and using Theorem 2.2, it is now possible to compute any joint probability of dominoes. We choose to compute the probability distribution of southern dominoes (or equivalently dimers) in various locations of the Aztec diamond.

The southern domino process is defined as follows: fix $r$, $1 \le r \le n$. With a southern domino on the line $y = r$, we mean a dimer with a white vertex $w = (2s-1, 2r)$ and a black vertex $b = (2s, 2r+1)$ for some $s \in \{1, \dots, n\}$, and we say that the southern domino is located at $s$ on the line $y = r$. The southern dominoes form a determinantal process by Theorem 2.2, and in particular so do the southern dominoes on the line $y = r$ with the kernel given by the following lemma.

LEMMA 2.5. *A kernel of the determinantal process given by the positions of the southbound dominoes on a fixed line $y = r$ in a random tiling of an Aztec diamond is*

$$L(x_1, x_2) := -\frac{1}{(2\pi i)^2} \int_{\mathcal{E}_1} dz \int_{\mathcal{E}_2} dw \, \frac{w^{x_2}}{z^{x_1}} \frac{(a+z)^r (az-1)^{n-r}}{(aw-1)^{n-r}(a+w)^{r+1}(w-z)}. \tag{2.18}$$

PROOF. From Theorem 2.2, the kernel of the southern dominoes along a fixed line $y = r$ is given by (up to conjugation)

$$K(b, \tilde{w}) K^{-1}(w, b), \tag{2.19}$$

where we set $w = (2x_1 - 1, 2r)$, $\tilde{w} = (2x_2 - 1, 2r)$ and $b = (2x_2, 2r+1)$. From Theorem 2.3, we have a formula for each entry of $K^{-1}$ and in the case $x_1 < x_2$, we have that

$$f_2(w, b) = \frac{(-1)^{((x_1+x_2)/2)+r}}{2\pi i} \int_{|z|=\epsilon} \frac{(1/a+z)^{x_2-x_1-1}}{1/a+a+z} \, dz = 0 \tag{2.20}$$

because the integrand is analytic at $z = 0$. From the above equation, we have

$$\begin{aligned} &K(b, \tilde{w}) K^{-1}(w, b) \\ &\quad = (-1)^{(2x_2+2r)/2} \frac{(-1)^{((x_1+x_2)/2)+r}}{(2\pi i)^2} \\ &\qquad \times \int_{\mathcal{E}_1} \int_{\mathcal{E}_2} \frac{w^{x_2}}{z^{x_1}} \frac{(a+z)^r (az-1)^{n-r}}{(aw-1)^{n-r}(a+w)^{r+1}(w-z)} \, dw \, dz. \end{aligned} \tag{2.21}$$

In the above equation, the sign is equal to $(-1)^{(x_1+3x_2)/2} = -(-1)^{(x_2-x_1)/2}$. We can remove a factor of $(-1)^{(x_2-x_1)/2}$ from the above equation by a conjugation which gives (2.18). □

2.2.2. *Thickening and thinning determinantal point processes*. Consider a determinantal point process $\nu$ on a space $\Lambda$ with correlation kernel $\mathbb{K}$. Let $0 \le \alpha \le 1$ and consider the point process obtained by removing each point in the process independently with probability $1-\alpha$. We will call this new point process the *thinned determinantal point process* with correlation kernel $\mathbb{K}$ and parameter $\alpha$. A way of modifying the original point process to obtain a point process with multiple points is by taking each point in the process $\nu$ independently with multiplicity $m$, where $m$ is a geometric random variable with parameter $\beta$, $\mathbb{P}[m=k] = (1-\beta)\beta^{k-1}$, $k \ge 1$. We will call this (multiple) point process a *thickened determinantal point process* with correlation kernel $\mathbb{K}$ and parameter $\beta$.

PROPOSTION 2.6. *The thinned determinantal point process $\{x_j\}$ with correlation kernel $\mathbb{K}$ and parameter $\alpha$ is again a determinantal point process with correlation kernel $\alpha\mathbb{K}$, that is,*

$$\mathbb{E}\big[e^{-\sum_j \psi(x_j)}\big] = \det(I - \phi\alpha\mathbb{K}\mathbb{I}_A), \tag{2.22}$$

*for every $\psi \in C_c^+(\Lambda)$, $\phi = 1 - e^{-\psi}$ and $A = \operatorname{supp}\psi = \operatorname{supp}\phi$. With the same notation the thickened determinantal point process with kernel $\mathbb{K}$ and parameter $\beta$ is characterized by*

$$\mathbb{E}\big[e^{-\sum_j \psi(x_j)}\big] = \det\left(I - \frac{\phi}{1-\beta+\beta\phi}\mathbb{K}\mathbb{I}_A\right), \tag{2.23}$$

*where $\{x_j\}$ is now the multi-set of points of the process.*

We will prove the proposition in Section 4. Note that the thickened process is no longer a determinantal point process since determinantal point processes are always simple point processes.

2.2.3. *Asymptotic coordinates*. Here, we introduce the asymptotic coordinates of the unfrozen region. As $n \to \infty$, for the (rescaled) Aztec diamond with corners $(0,0)$, $(1,0)$, $(0,1)$ and $(1,1)$, the boundary between the frozen and unfrozen regions is an ellipse [8] whose equation is given by

$$\frac{(v-u)^2}{1-p} + \frac{(u+v-1)^2}{p} = 1, \tag{2.24}$$

where $u \in [0,1]$ is the horizontal coordinate, $v \in [0,1]$ is the vertical coordinate and $p = 1/(1+a^2)$. We let $\mathcal{D} \subset \mathbb{R}^2$ be the area bounded by the ellipse given in (2.24).

For our results on the edge, we are interested in the boundary of the ellipse. This is given by

$$v = 1 - u \pm 2\sqrt{(1-p)p(1-u)u} + p(2u-1). \tag{2.25}$$

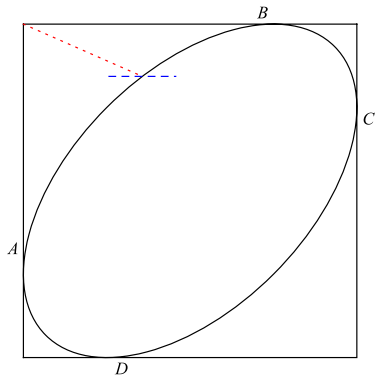


FIG. 5. *This figure shows the intersection of the limiting ellipse with the red dotted line given by* $v = 1 - k^2 u$. *The southern dominoes on the blue dashed line represent the southern domino process. The northern boundary lies between A and B and the southern boundary between C and D.*

The arctic ellipse can be parametrized by $(u(k), v(k))$, where $v(k) = 1 - k^2 u(k)$ and

$$u(k) = \frac{1}{(1+a^2)(1+k^2) + 2a\sqrt{1+a^2}k}. \tag{2.26}$$

We will be interested in two parts of the boundary. The part where $k > 0$ will be called the *northern boundary*, and the part where $k \in (-a^{-1}(1+a^2)^{1/2}, -a(1+a^2)^{-1/2}) = (-1/\sqrt{1-p}, -\sqrt{1-p})$ the *southern boundary*. See Figure 5 for an example of the northern and southern boundaries and an explanation of the geometric meaning of $k$.

2.2.4. *Results on the southern domino process.* Here, we consider the behavior of the southern domino process along the northern and southern boundaries. Along the southern boundary the southern domino process is almost dense, and we have to consider the dual process, the process of holes, instead. If we think of the locations in $1, \dots, n$ of the southern dominoes on the line $y = r$ as positions of particles, then the empty spaces, the holes, also form a determinantal point process with a kernel $I - L$, where $L$ is the kernel for the particles.

In our scaling limits we will obtain the *Airy kernel point process* which is a determinantal point process with kernel

$$K_{\mathrm{Ai}}(x, y) = \int_0^\infty \mathrm{Ai}(x+t)\,\mathrm{Ai}(y+t)\,dt. \tag{2.27}$$

Set

$$\beta = -a\big(a + k\sqrt{1+a^2}\big), \tag{2.28}$$

$$\alpha = \frac{1}{1-\beta} = \frac{1}{1+a^2+ak\sqrt{1+a^2}}, \tag{2.29}$$

and let $\lambda > 0$ be given by

$$\lambda^3 = \pm \frac{a(a + k\sqrt{1+a^2})^2}{(1+a^2)(ak^2 + k\sqrt{1+a^2})((1+a^2)(1+k^2) + 2ak\sqrt{1+a^2})} \tag{2.30}$$

with the plus sign for $k > 0$ and the minus sign for $k < 0$.

THEOREM 2.7. *Let $a > 0$ be fixed, and let $\lambda$ be given by (2.30), $\alpha$ by (2.29) and $\beta$ by (2.28). Furthermore, let $\{x_j\}$ be the positions of the southern dominoes on the line $y = [(1 - k^2 u(k)n]$, where $u(k)$ is given by (2.26). Consider a fixed $k > 0$. Then the rescaled southern domino process at the northern boundary,*

$$\xi_j = \frac{u(k)n - x_j}{\lambda n^{1/3}},$$

*converges weakly to the thinned Airy kernel point process with parameter $\alpha$.*

*Next, consider a fixed $k \in (-a^{-1}(1+a^2)^{1/2}, -a(1+a^2)^{-1/2})$. Let $\{y_j\}$ be the positions of the holes in the south domino process, that is, the dual south domino process, at the southern boundary. The rescaled point process*

$$\xi_j = \frac{y_j - u(k)n}{\lambda n^{1/3}}$$

*converges weakly to the thickened Airy kernel point process with parameter $\beta$.*

Successive independent thinning and rescaling of a point process typically has a Poisson point process as its limit. If $a$ tends to infinity, we see that the thinning parameter of the thinned Airy kernel $\alpha$ tends to zero. Hence we can expect that if we let $a$ tend to infinity with $n$ (but not too fast), the southern domino point process close to the northern boundary should converge to a Poisson process. This leads to the next theorem.

THEOREM 2.8. *Fix $k > 0$, and let $a = a(n)$, where $a(n) \to \infty$ but $a(n)/n^{1/10} \to 0$ as $n \to \infty$. Set $c(a) = \pi^{2/3}(1 + 1/k)^{1/3} a^{2/3}$, and let $\{x_j\}$ be the positions of the south dominoes on the line $y = [n(1 - k^2 u(k))]$. Then the rescaled point process*

$$\xi_j = \frac{u(k)n + c(a)n^{1/3} - x_j}{c(a)n^{1/3}} \tag{2.31}$$

*converges weakly to a Poisson process with density $\rho(\xi) = \sqrt{(1-\xi)_+}$.*

The condition on the allowed growth of $a(n)$ is certainly not optimal but is an outcome of the proof. A similar result holds for the thinned Airy kernel point process on $\mathbb{R}$: if the thinning parameter is sent to zero, the Airy kernel can be rescaled to a Poisson point process on $\mathbb{R}$ which has a square root drop off. This result actually follows from the proof of Theorem 2.8. Thus we can think of the thinned Airy kernel point process as being an intermediate kernel between the Airy kernel and the Poisson point processes with density $\sqrt{(1-\xi)_+}$.

REMARK 1. We could also consider the behavior of the leftmost southern domino along the northern boundary. For a fixed $a$ we should get convergence to the last particle distribution for the thinned Airy kernel point process, $\det(I - \alpha K_{\mathrm{Ai}})_{L^2(\xi,\infty)}$. When $a$ goes to infinity with $n$, but not too quickly, we expect instead get one of the classical extreme value distributions in the limit, namely the last particle distribution in a Poisson process with density $\sqrt{(1-\xi)_+}$. We will not give the technical details that are required to prove these natural conjectures, but it should be possible by developing the proof of Theorem 2.8 further.

2.3. *Bulk fluctuations*. An account of *local Gibbs measures* for tiling models can be found in [33] and [31].

For all doubly periodic bipartite weighted dimer models embedded in the plane, in [33] the authors found that the dimer model is a Gibbs measure, gave an explicit method to compute the entries of the inverse Kasteleyn matrix embedded in the plane and the complete phase portrait. The results from [33] rely on using the smallest nonrepeating unit of the graph called the *fundamental domain*. For the graph considered in this paper, the fundamental domain has one black vertex and one white vertex. In order to describe the Gibbs measure, the authors of [33] introduced magnetic coordinates $(B_x, B_y)$, where one increases the energy by $e^{B_x}$ or $e^{B_y}$ if one passes to the neighboring fundamental domain to the left or above. Conversely, if one passes to the fundamental domain to the right or below, one decreases the energy by $e^{B_x}$ or $e^{B_y}$. These magnetic coordinates are related to the average slope; that is, one can compute the Gibbs measures for different slopes; see [33].

We choose the fundamental domain of the graph embedded in the plane to be given by a white vertex, an edge in the direction $+e_2$ and its incident black vertex and the remaining edges incident to these vertices. To make the following computations and formulas simpler and since the dimer model is independent of the chosen Kasteleyn orientation, we choose the Kasteleyn orientation which multiplies the Kasteleyn orientation given in Section 2.1.4 by $(-1)$ at the black vertices $(b_1, b_2)$ where $b_1 + b_2 \bmod 4 = 3$. Figure 6 shows our choice of fundamental domain.

We denote the Gibbs measure of the model on this graph by $\mu_a(B_x, B_y)$ where $(B_x, B_y)$ is described above. Suppose that $(2\alpha_1 + 1, 2\alpha_2)$ is a white vertex, and $(2\beta_1, 2\beta_2 + 1)$ is a black vertex for $\alpha_1, \alpha_2, \beta_1, \beta_2 \in \mathbb{Z}$. Using techniques from [33] one can find the entries of the inverse of the (infinite) Kasteleyn matrix, denoted by $K_\mu^{-1}$, and they are given by

$$\begin{aligned} &K_\mu^{-1}\big((2\alpha_1+1, 2\alpha_2), (2\beta_1, 2\beta_2+1)\big) \\ &\quad = \frac{1}{(2\pi i)^2} \int_{|z|=1} \int_{|w|=1} \frac{z^{\alpha_1-\beta_1} w^{\beta_2-\alpha_2}}{P(ze^{B_x}, we^{B_y})} \frac{dw}{w} \frac{dz}{z}, \end{aligned} \tag{2.32}$$

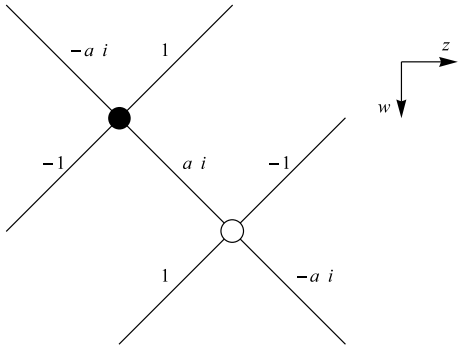


FIG. 6. *The fundamental domain.*

where $P(z, w)$ is the so-called *characteristic polynomial*. For the above graph embedded in the torus with the above edge weights and Kasteleyn orientation, the characteristic polynomial is given by

$$P(z, w) = ai - z^{-1} + w^{-1} - aiw^{-1}z^{-1}. \tag{2.33}$$

THEOREM 2.9. *Choose the rescaling so that the white vertices are given by*

$$(x_1, x_2) = \big([2\xi_1 n] + 2\alpha_1 + 1, [2\xi_2 n] + 2\alpha_2\big)$$

*and the black vertices are given by*

$$(y_1, y_2) = \big([2\xi_1 n] + 2\beta_1, [2\xi_2 n] + 2\beta_2 + 1\big)$$

*for $\xi_1, \xi_2 \in \mathcal{D}_c \subset \mathcal{D}$ compact and for $\alpha_1, \alpha_2, \beta_1, \beta_2 \in \mathbb{Z}$ where $\mathcal{D}$ is the area bounded by the ellipse in (2.24). Then the measure on domino tilings converges weakly to $\mu_a(\log r_1, \log r_2)$ where $\mu_a$ is defined above and*

$$r_i = \sqrt{\xi_i/(1 - \xi_i)} \qquad \text{for } i \in \{1, 2\}. \tag{2.34}$$

Similar results for certain classes of lozenge tilings have been obtained in [4] and [38].

2.4. *Overview of the paper.* The rest of the paper is organized as follows. In Section 3, we prove Theorem 2.3 and Proposition 2.4. In Section 4, we give the proofs of Theorems 2.7 and 2.8. The proof of Theorem 2.9 is given in Section 5. We conclude with a brief discussion of the height function fluctuation in Section 6.

## 3. Discrete setting.

3.1. *Proof of Theorem* 2.3. Before giving the proof of Theorem 2.3, we introduce some notation: for $x = (x_1, x_2) \in \mathbb{W}$ and $y = (y_1, y_2) \in \mathbb{B}$, let

$$c_1(w, z, x, y) = (-1)^{(y_1+y_2+x_1+x_2)/4} \times \frac{w^{y_1/2}(a+z)^{x_2/2}(az-1)^{(2n-x_2)/2}}{z^{(x_1+1)/2}(w-z)(aw-1)^{(2n+1-y_2)/2}(a+w)^{(y_2+1)/2}}, \tag{3.1}$$

$$c_2(z, x, y) = (-1)^{(y_1+y_2+x_1+x_2)/4} a^{(y_2-x_2-1)/2} \times \frac{z^{(y_2-x_2-1)/2}(1/a+z)^{(y_1-x_1-1)/2}}{(1/a+a+z)^{(y_2-x_2+1)/2}} \tag{3.2}$$

and

$$\tilde{c}_2(w, x, y) = (-1)^{(y_1+y_2+x_1+x_2)/4} w^{(y_1-x_1-1)/2} \times (aw-1)^{(y_2-x_2-1)/2}(a+w)^{(x_2-y_2-1)/2}. \tag{3.3}$$

We have chosen the three functions above so that

$$\frac{1}{(2\pi i)^2} \int_{\mathcal{E}_2} \int_{\mathcal{E}_1} c_1(w, z, x, y)\, dz\, dw = f_1(x, y) \tag{3.4}$$

and

$$\frac{1}{2\pi i} \int_{\mathcal{E}_1} c_2(z, x, y)\, dz = \frac{1}{2\pi i} \int_{\mathcal{E}_2} \tilde{c}_2(w, x, y)\, dw = f_2(x, y), \tag{3.5}$$

where the contours $\mathcal{E}_1$ and $\mathcal{E}_2$ are given in the statement of Theorem 2.3, and the functions $f_1(x, y)$ and $f_2(x, y)$ are given in equations (2.15) and (2.16), respectively. Note that $c_2$ is obtained from $\tilde{c}_2$ by the change of variables $z \mapsto w - 1/a$ and

$$\lim_{z \to w} (w - z) c_1(w, z, x, y) = \tilde{c}_2(w, x, y). \tag{3.6}$$

PROOF OF THEOREM 2.3. For the proof, we set $x = (x_1, x_2)$ and $y = (y_1, y_2)$ with $x, y \in \mathbb{B}$. We keep the same notation throughout the proof. The matrix $K^{-1}$ is uniquely determined by the specific choice of the Kasteleyn matrix, $K$, which means we need to verify the equation $K \cdot K^{-1} = \mathbb{I}$. We can expand out $K \cdot K^{-1}$ entry-wise. For $x, y \in \mathbb{B}$, we obtain

$$K \cdot K^{-1}(x, y) = \sum_{w \in \mathbb{W}} K(x, w) K^{-1}(w, y) = \sum_{w \sim x, w \in \mathbb{W}} K(x, w) K^{-1}(w, y), \tag{3.7}$$

where $w \sim x$, $w \in \mathbb{W}$ means that $w \in \mathbb{W}$ and $w$ is a nearest neighbored vertex to $x$. Using the entries of the Kasteleyn matrix given in (2.11), we can rewrite (3.7) and compare with the identity matrix which gives an entry-wise expansion of the

equation $K \cdot K^{-1} = \mathbb{I}$. This is the equation we must verify to prove Theorem 2.3. That is, we must verify

$$\begin{aligned}(-1)^{(x_1+x_2-1)/2}&\big(K^{-1}(x+e_1,y)\mathbb{I}_{x_1<2n} - K^{-1}(x-e_1,y)\mathbb{I}_{x_1>0}\\ &- aiK^{-1}(x+e_2,y)\mathbb{I}_{x_1>0} + aiK^{-1}(x-e_2,y)\mathbb{I}_{x_1<2n}\big)\\ &= \mathbb{I}_{x=y},\end{aligned} \tag{3.8}$$

where $x = (x_1, x_2)$, $y \in \mathtt{B}$ and

$$\mathbb{I}_{x_1>0} = \begin{cases} 1, & \text{if } x_1 > 0,\\ 0, & \text{otherwise.}\end{cases} \tag{3.9}$$

Note that the indicator functions in (3.8) account for $x$ on the boundary of the Aztec diamond. In order to verify (3.8), there are three cases to consider for $x = (x_1, x_2)$: $0 < x_1 < 2n$, $x_1 = 0$ and $x_1 = 2n$.

For $0 < x_1 < 2n$, the left-hand side of (3.8) is equal to

$$\begin{aligned}(-1)^{(x_1+x_2-1)/2}&\big(K^{-1}(x+e_1,y) - K^{-1}(x-e_1,y)\\ &- aiK^{-1}(x+e_2,y) + aiK^{-1}(x-e_2,y)\big).\end{aligned} \tag{3.10}$$

We first substitute $f_1$ into the above expression. For this expression, we will manipulate the integrand of $f_1$ which is given by $c_1$ by (3.4). We find after some simplification,

$$\begin{aligned}&(-1)^{(x_1+x_2-1)/2}\big(c_1(w,z,x+e_1,y) - c_1(w,z,x-e_1,y)\\ &\qquad - aic_1(w,z,x+e_2,y) + aic_1(w,z,x-e_2,y)\big)\\ &\quad = (-1)^{(x_1+x_2-1)/2}\\ &\qquad \times \big(c_1\big(w,z,(x_1+1,x_2+1),y\big) - c_1\big(w,z,(x_1-1,x_2-1),y\big)\\ &\qquad\quad - aic_1\big(w,z,(x_1-1,x_2+1),y\big) + aic_1\big(w,z,(x_1+1,x_2-1),y\big)\big)\\ &\quad = (-1)^{(x_1+x_2-1)/2}\\ &\qquad \times c_1(w,z,x+e_1,y)\left(1 - az + \frac{a(-1+az)}{a+z} + \frac{z(-1+az)}{a+z}\right) = 0.\end{aligned} \tag{3.11}$$

Note that this relation holds for $0 \le x_1 \le 2n$. Integrating both sides of the above equation with respect to $z$ and $w$ over the contours $\mathcal{E}_1$ and $\mathcal{E}_2$, respectively, and using (3.4), we find that

$$\begin{aligned}(-1)^{(x_1+x_2-1)/2}&\big(f_1(x+e_1,y) - f_1(x-e_1,y)\\ &- aif_1(x+e_2,y) + aif_1(x-e_2,y)\big) = 0.\end{aligned} \tag{3.12}$$

To substitute $f_2$ into the expression given in (3.10), we have to consider $x_1 = y_1$ and $x_1 \ge y_1 + 2$ separately due to the split expression of $K^{-1}$. For $x_2 \ge y_1 + 2$, all

four terms of $f_2$ are present in (3.10) and so using (3.6), (3.11) and (3.5) we find

$$\begin{aligned}-(-1)^{(x_1+x_2-1)/2}\big(&f_2(x+e_1,y)-f_2(x-e_1,y)\\&-aif_2(x+e_2,y)+aif_2(x-e_2,y)\big)=0.\end{aligned}\tag{3.13}$$

We now substitute $f_2$ into (3.10) for the case $x_1 = y_1$. We obtain

$$\begin{aligned}-(-1)^{(x_1+x_2-1)/2}\big(&f_2\big((x_1+1,x_2+1),(x_1,y_2)\big)\\&+aif_2\big((x_1+1,x_2-1),(x_1,y_2)\big)\big).\end{aligned}\tag{3.14}$$

We first manipulate the integrand of the above equation using (3.5) which gives

$$\begin{aligned}&-(-1)^{(x_1+x_2-1)/2}\big(c_2\big(z,(x_1+1,x_2+1),(x_1,y_2)\big)\\&\qquad+aic_2\big(z,(x_1+1,x_2-1),(x_1,y_2)\big)\big)\\&\quad=-(-1)^{(x_1+x_2-1)/2}c_2\big(z,(x_1+1,x_2+1),(x_1,y_2)\big)\bigg(1+\frac{a^3z}{1+a^2+az}\bigg)\\&\quad=-(-1)^{(x_1+x_2-1)/2}c_2\big(z,(x_1+1,x_2+1),(x_1,y_2)\big)\bigg(\frac{(1+a^2)(1+az)}{1+a^2+az}\bigg)\\&\quad=-(-1)^{(3x_1+3x_2+y_1+y_2)/4}a^{(y_2-x_2-2)/2}\\&\qquad\times(1+a^2)z^{(y_2-x_2-2)/2}\bigg(\frac{1}{a}+a+z\bigg)^{(x_2-y_2-2)/2}.\end{aligned}\tag{3.15}$$

We now integrate with respect to $z$ over the contour $\mathcal{E}_1$, and we obtain

$$\begin{aligned}&-(-1)^{(x_1+x_2-1)/2}\big(f_2\big((x_1+1,x_2+1),(x_1,y_2)\big)\\&\qquad+aif_2\big((x_1+1,x_2-1),(x_1,y_2)\big)\big)\\&\quad=-\frac{(-1)^{(3x_1+3x_2+y_1+y_2)/4}}{2\pi i}\\&\qquad\times\int_{\mathcal{E}_1}a^{(y_2-x_2-2)/2}(1+a^2)z^{(y_2-x_2-2)/2}\bigg(\frac{1}{a}+a+z\bigg)^{(x_2-y_2-2)/2}dz\\&\quad=\begin{cases}-(-1)^{(x_1+x_2)}, & x_2=y_2,\\ 0, & \text{otherwise}\end{cases}\end{aligned}\tag{3.16}$$

by Lemma 3.1 below. Because $x_1 + x_2$ is always odd, we conclude

$$\begin{aligned}-(-1)^{(x_1+x_2-1)/2}\big(&f_2\big((x_1+1,x_2+1),(x_1,y_2)\big)\\&+aif_2\big((x_1+1,x_2-1),(x_1,y_2)\big)\big)=\mathbb{I}_{x_2=y_2}.\end{aligned}\tag{3.17}$$

Note that by our method of computation, the above relation is valid for $0 \le x_1 \le 2n$. This means we have computed (3.10) for $0 < x_1 < 2n$ and so from (3.12),

(3.13) and (3.17), we have obtained for $0 < x_1 < 2n$,

$$(-1)^{(x_1+x_2-1)/2}\big(K^{-1}(x+e_1,y)-K^{-1}(x-e_1,y) - ai\,K^{-1}(x+e_2,y)+ai\,K^{-1}(x-e_2,y)\big)=\mathbb{I}_{x=y}. \tag{3.18}$$

For $x=(0,x_2)$, we have that the left-hand side of (3.8) is equal to

$$(-1)^{(x_2-1)/2}\big(K^{-1}(x+e_1,y)+ai\,K^{-1}(x-e_2,y)\big). \tag{3.19}$$

Before we substitute $f_1$ into (3.19), notice that

$$f_1\big((-1,w_2),(y_1,y_2)\big)=0 \tag{3.20}$$

for $w_2 \bmod 2 = 0$ because there is no residue at $z=0$ in (2.15) in this case. Since (3.11) holds for $x$ (including those outside of the Aztec diamond) which means that the relation in (3.12) holds for any values of $x$, we can write out (3.11) with $x_1=0$, integrate over $z$ and $w$ over the contours $\mathcal{E}_1$ and $\mathcal{E}_2$, respectively, noting (3.20), and use (3.4) to obtain

$$\begin{aligned}&(-1)^{(x_2-1)/2}\big(f_1\big((1,x_2+1),y\big)-f_1\big((-1,x_2-1),y\big)\\ &\qquad -aif_1\big((-1,x_2+1),y\big)+aif_1\big((1,x_2-1),y\big)\big)\\ &=(-1)^{(x_2-1)/2}\big(f_1(x+e_1,y)+aif_1(x-e_2,y)\big)=0\end{aligned} \tag{3.21}$$

for $x=(0,x_2)$. When we substitute $f_2$ into (3.19), we only need to consider the case $y_1=0$ because of the split definition of $K^{-1}$, and so using (3.17) (because the equation is valid for $0\le x_1\le 2n$), we obtain

$$-(-1)^{(x_2-1)/2}\big(f_2\big((1,x_2+1),(0,y_2)\big) + aif_2\big((1,x_2-1),(0,y_2)\big)\big)=\mathbb{I}_{x_2=y_2}. \tag{3.22}$$

Adding (3.21) and (3.22), we find

$$(-1)^{(x_2-1)/2}\big(K^{-1}(x+e_1,y)+ai\,K^{-1}(x-e_2,y)\big)=\mathbb{I}_{x=y} \tag{3.23}$$

for $x=(0,x_2)$.

For $x=(2n,x_2)$, we have that the left-hand side of (3.8) is equal to

$$(-1)^{(2n+x_2-1)/2}\big(-K^{-1}(x-e_1,y)-ai\,K^{-1}(x+e_2,y)\big). \tag{3.24}$$

For $x=(2n,x_2)$, we perform the following computation:

$$\begin{aligned}&(-1)^{(2n+x_2-1)/2}\big(-f_1\big((2n-1,x_2-1),y\big)-aif_1\big((2n-1,x_2+1),y\big)\big)\\ &\quad=-\frac{(-1)^{(2n+x_2-1)/2}}{(2\pi i)^2}\int_{\mathcal{E}_2}\int_{\mathcal{E}_1}c_1\big(w,z,(2n-1,x_2-1),y\big) + aic_1\big(w,z,(2n-1,x_2+1),y\big)\,dz\,dw\end{aligned} \tag{3.25}$$

$$
\begin{aligned}
&= -\frac{(-1)^{(2n+x_2-1)/2}}{(2\pi i)^2} \\
&\quad \times \int_{\mathcal{E}_2}\int_{\mathcal{E}_1} c_1\big(w, z, (2n-1, x_2-1), y\big)\Big(1 - \frac{a(a+z)}{az-1}\Big)\, dz\, dw \\
&= -\frac{(-1)^{(2n+x_2-1)/2}}{(2\pi i)^2} \\
&\quad \times \int_{\mathcal{E}_2}\int_{\mathcal{E}_1} c_1\big(w, z, (2n-1, x_2-1), y\big)\Big(\frac{1+a^2}{az-1}\Big)\, dz\, dw \\
&= -\frac{(-1)^{(2n+x_2-1)/2}}{(2\pi i)^2}\int_{\mathcal{E}_2} \tilde{c}_2\big(w, (2n-1, x_2-1), y\big)\frac{1+a^2}{1-aw}\, dw \\
&= -(-1)^{(2n+x_2-1)/2}\big(f_2\big((2n-1, x_2-1), y\big) + ai f_2\big((2n-1, x_2+1), y\big)\big),
\end{aligned}
$$

where the fourth line to the fifth line follows from the fact that the integrand in the fourth line is a polynomial of degree $n-1$ in the numerator and a polynomial of degree $n+1$ in the denominator with respect to $z$, and so we can push the contour through infinity which picks up a residue at $z = w$. The sixth line follows from the fifth line because

$$
\begin{aligned}
&\tilde{c}_2\big(w, (2n-1, x_2-1), y\big) + ai\tilde{c}_2\big(w, (2n-1, x_2+1), y\big) \\
&\qquad = \tilde{c}_2\big(w, (2n-1, x_2-1), y\big)\Big(1 - \frac{a(a+w)}{-1+aw}\Big) \\
&\qquad = \tilde{c}_2\big(w, (2n-1, x_2-1), y\big)\frac{1+a^2}{1-aw}
\end{aligned} \tag{3.26}
$$

and integrating over $\mathcal{E}_2$ using (3.5). For $x_1 = 2n$ and $y_1 < 2n$, we have that (3.24) is equal to

$$
\begin{aligned}
&-(-1)^{(2n+x_2-1)/2}\big(f_1(x-e_1, y) - f_2(x-e_1, y) \\
&\qquad + ai\big(f_1(x+e_2, y) - f_2(x+e_2, y)\big)\big) = 0
\end{aligned} \tag{3.27}
$$

by (3.25). For $x = (2n, x_2)$ and $y_1 = 2n$, using (3.25), (3.24) is equal to

$$
\begin{aligned}
&-(-1)^{(2n+x_2-1)/2}\big(f_1(x-e_1, y) + ai f_1(x+e_2, y)\big) \\
&\qquad = -(-1)^{(2n+x_2-1)/2}\big(f_2(x-e_1, y) + ai f_2(x+e_2, y)\big) \\
&\qquad = (-1)^{(2n+x_2-1)/2}\big(f_2(x+e_1, y) + ai f_2(x-e_2, y)\big) \\
&\qquad = \mathbb{I}_{x=y}
\end{aligned} \tag{3.28}
$$

for $y = (2n, y_2)$ by using (3.13) and (3.17). From (3.27) and (3.28), we have evaluated (3.24) and have found

$$
(-1)^{(2n+x_2-1)/2}\big(-K^{-1}(x-e_1, y) - ai K^{-1}(x+e_2, y)\big) = \mathbb{I}_{x=y} \tag{3.29}
$$

for $x = (2n, x_2)$ and $y = (y_1, y_2)$. Equations (3.18), (3.23) and (3.29) means that we have verified (3.8). $\square$

LEMMA 3.1. *For $k \in \mathbb{Z}$,*

$$\frac{1}{2\pi i}\int_{|z|=1} z^{k-1}\left(\frac{1}{a}+a+z\right)^{-1-k} dz = \begin{cases} \dfrac{a}{1+a^2}, & k=0, \\ 0, & \text{otherwise}. \end{cases} \tag{3.30}$$

PROOF. For $k = 0$, the left-hand side of (3.30) is equal to

$$\frac{1}{2\pi i}\int_{|z|=1} \frac{1}{z((1/a)+a+z)}\, dz = \frac{a}{1+a^2}. \tag{3.31}$$

When $k > 0$, the integrand in (3.30) is analytic at $z = 0$ and so the left-hand side of (3.30) is zero. When $k < 0$, we can move the contour to a small circle around $-(a + 1/a)$ and use the fact that the integrand is analytic inside. $\square$

3.2. *Guessing $K^{-1}$.* As mentioned above in [22], the author used a particle system formed from the zig-zag particles and obtained a formula for the correlation kernel. From this correlation kernel, we could guess an expression for the inverse Kasteleyn matrix which is verified to be correct in the previous section. Here, we describe the steps we used to obtain the guess.

Let $w \in \mathtt{W}$ and $b \in \mathtt{B}$. Recall that there is a blue particle at $w$ if and only if a dimer covers $(w + e_1, w)$ or $(w + e_2, w)$ and that there is a red particle at $b$ if and only if a dimer covers $(b, b - e_1)$ or $(b, b - e_2)$. From (2.11) we see that if $w = (x_1, x_2)$, then

$$\begin{aligned} K(w+e_1, w) &= (-1)^{(x_1+x_2-1)/2}, \\ K(w+e_2, w) &= (-1)^{(x_1+x_2-1)/2} ai \end{aligned} \tag{3.32}$$

and if $b = (y_1, y_2)$, then

$$\begin{aligned} K(b, b-e_1) &= (-1)^{(y_1+y_2+1)/2}, \\ K(b, b-e_2) &= -(-1)^{(y_1+y_2+1)/2} ai. \end{aligned} \tag{3.33}$$

It follows from Theorem 2.2 that

$$\begin{aligned} &\mathbb{P}[\text{There are particles at } w \text{ and } b] \\ &= \sum_{r_1,r_2=1}^{2} K(w+e_{r_1}, w) K(b, b-e_{r_2}) \\ &\qquad \times \begin{vmatrix} K^{-1}(w, w+e_{r_1}) & K^{-1}(w, b) \\ K^{-1}(b-e_{r_2}, w+e_{r_1}) & K^{-1}(b-e_{r_2}, b) \end{vmatrix} \end{aligned} \tag{3.34}$$

$$= \begin{vmatrix} \displaystyle\sum_{r=1}^{2} K^{-1}(w, w+e_r)K(w+e_r, w) & K^{-1}(w, b) \\ \displaystyle\sum_{r_1,r_2=1}^{2} K^{-1}(b-e_{r_2}, w+e_{r_1})K(w+e_{r_1}, w)K(b, b-e_{r_2}) & \displaystyle\sum_{r=1}^{2} K^{-1}(b-e_r, b)K(b, b-e_r) \end{vmatrix}.$$

In (3.34), we have $w = (x_1, x_2)$, $b = (y_1, y_2)$ and if $(v_1, v_2)$, the particle coordinates, are related to $(x_1, x_2)$ by (2.7) and $(v_1, v_2)$ in the same way to $(y_1, y_2)$, then we get, using the particle kernel (2.8) and the result in [22] that

$$\begin{aligned} &\mathbb{P}[\text{There are particles at } w \text{ and } b] \\ &= \begin{vmatrix} K_n(u_1, u_2; u_1, u_2) & K_n(u_1, u_2; v_1, v_2) \\ K_n(v_1, v_2 l u_1, u_2) & K_n(v_1, v_2 l v_1, v_2) \end{vmatrix}. \end{aligned} \tag{3.35}$$

Comparing (3.34) and (3.35), we see that it is reasonable to expect that

$$\begin{aligned} &K^{-1}\big((x_1, x_2), (y_1, y_2)\big) \\ &\quad = c(x_1, x_2; y_1, y_2)K_n(u_1, u_2; v_1, v_2) \end{aligned} \tag{3.36}$$

or

$$\begin{aligned} &K^{-1}\big((x_1, x_2), (y_1, y_2)\big) \\ &\quad = c(x_1, x_2; y_1, y_2)K_n(v_1, v_2; u_1, u_2) \end{aligned} \tag{3.37}$$

with some appropriate, hopefully simple function $c$ which could perhaps be just a sign factor. Here, one has to make some guesses and it turns out, a posteriori, that (3.37) is the right choice and that

$$c(x_1, x_2; y_1, y_2) = -(-1)^{(x_1-x_2+y_1-y_2+2)/4} \tag{3.38}$$

for our choice of Kasteleyn orientation. Thus we write

$$\begin{aligned} &K^{-1}\big((x_1, x_2), (y_1, y_2)\big) \\ &\quad = -(-1)^{(x_1-x_2+y_1-y_2+2)/4} K_n\left(y_2, \frac{y_2-y_1+1}{2}; x_2, \frac{x_2-x_1+1}{2}\right). \end{aligned} \tag{3.39}$$

3.3. *Proof of Proposition 2.4.* We will show that the right-hand side of (2.17) gives the corresponding entry of the inverse Kasteleyn matrix.

Write $y_2 = 2r - 1$ and $x_2 = 2s$. From (2.9), we see that

$$\begin{aligned}
&\widetilde{K}_n\Big(y_2, \frac{y_2 - y_1 + 1}{2}; x_2, \frac{x_2 - x_1 + 1}{2}\Big) \\
&\quad = \frac{1}{(2\pi i)^2} \\
&\qquad \times \int_{\gamma_{r_1}} \frac{dw}{w} \int_{\gamma_{r_2}} \frac{dz}{z} \frac{z^{(x_2 - x_1 + 1)/2}(1 - az)^{n - (x_2/2)}(1 + a/z)^{(x_2)/2}}{w^{(y_2 - y_1 + 1)/2}(1 - aw)^{n - ((y_2+1)/2) + 1}(1 + a/w)^{(y_2+1)/2}} \\
&\qquad\qquad \times \frac{w}{w - z} \\
&\quad = \frac{(-1)^{(y_2 - x_2 - 1)/2}}{(2\pi i)^2} \\
&\qquad \times \int_{\gamma_{r_1}} \frac{dw}{w} \int_{\gamma_{r_2}} \frac{dz}{z} \frac{w^{(y_1)/2}(az - 1)^{(2n - x_2)/2}(z + a)^{(x_2)/2}}{z^{(x_1+1)/2}(aw - 1)^{((2n - y_2 + 1)/2) + 1}(w + a)^{(y_2+1)/2}} \\
&\qquad\qquad \times \frac{1}{w - z} \\
&\quad = \frac{(-1)^{(y_2 - x_2 - 1)/2}}{(2\pi i)^2} \\
&\qquad \times \int_{\mathcal{E}_2} \frac{dw}{w} \int_{\mathcal{E}_1} \frac{dz}{z} \frac{w^{(y_1)/2}(az - 1)^{(2n - x_2)/2}(z + a)^{(x_2)/2}}{z^{(x_1+1)/2}(aw - 1)^{((2n - y_2 + 1)/2) + 1}(w + a)^{(y_2+1)/2}} \\
&\qquad\qquad \times \frac{1}{w - z},
\end{aligned} \tag{3.40}$$

where the last equality follows by deforming $\gamma_{r_2}$ to $\mathcal{E}_2$ through infinity. Hence, we obtain

$$\begin{aligned}
&-(-1)^{(x_1 - x_2 + y_1 - y_2 + 2)/4} \widetilde{K}_n\Big(y_2, \frac{y_2 - y_1 + 1}{2}; x_2, \frac{x_2 - x_1 + 1}{2}\Big) \\
&\qquad = f_1(x, y).
\end{aligned} \tag{3.41}$$

Also, by (2.10) we have

$$\begin{aligned}
&\phi_{y_2, x_2}\Big(\frac{y_2 - y_1 + 1}{2}, \frac{x_2 - x_1 + 1}{2}\Big) \\
&\qquad = \frac{\mathbb{I}_{y_2 < x_2}}{2\pi i} \int_{\gamma_{r_1}} z^{((x_2 - x_1)/2) - ((y_2 - y_1)/2)} \frac{(1 - az)^{((y_2 + 1 - x_2)/2) - 1}}{(1 + a/z)^{(y_2 + 1 - x_2)/2}} \frac{dz}{z} \\
&\qquad = (-1)^{(y_2 - x_2 - 1)/2} \frac{\mathbb{I}_{y_2 < x_2}}{2\pi i} \int_{\gamma_{r_1}} z^{(y_1 - x_1 - 1)/2} \frac{(az - 1)^{(y_2 - x_2 - 1)/2}}{(z + a)^{(y_2 - x_2 + 1)/2}} dz
\end{aligned} \tag{3.42}$$

$$
\begin{aligned}
&= (-1)^{(y_2-x_2-1)/2} \frac{\mathbb{I}_{y_2<x_2}\mathbb{I}_{y_1<x_1}}{2\pi i} \\
&\quad \times \int_{\gamma_{r_1}} z^{(y_1-x_1-1)/2} \frac{(az-1)^{(y_2-x_2-1)/2}}{(z+a)^{(y_2-x_2+1)/2}}\, dz \\
&= (-1)^{(y_2-x_2-1)/2} \frac{\mathbb{I}_{y_2<x_2}\mathbb{I}_{y_1<x_1}}{2\pi i} \\
&\quad \times \int_{\mathcal{E}_2} z^{(y_1-x_1-1)/2} \frac{(az-1)^{(y_2-x_2-1)/2}}{(z+a)^{(y_2-x_2+1)/2}}\, dz \\
&= (-1)^{(y_2-x_2-1)/2} \frac{\mathbb{I}_{y_1<x_1}}{2\pi i} a^{(y_2-x_2-1)/2} \\
&\quad \times \int_{\mathcal{E}_1} z^{(y_2-x_2-1)/2} \frac{(1/a+z)^{(y_1-x_1-1)/2}}{(z+a+1/a)^{(y_2-x_2+1)/2}}\, dz.
\end{aligned}
$$

In the third equality, we use the fact that the integrand has no singularity inside $\gamma_1$ if $y_1 > x_1$ (and $y_1 = x_1$ is not possible). The fourth equality follows by deforming $\gamma_1$ to $\mathcal{E}_2$ through infinity. The last equality follows since the integrand has no singularity inside $\mathcal{E}_2$ if $y_2 > x_2$ and by making the shift $z \mapsto z + 1/a$. We see that

$$
\begin{aligned}
&-(-1)^{(x_1-x_2+y_1-y_2+2)/4} \phi_{y_2,x_2}\left(\frac{y_2-y_1+1}{2}, \frac{x_2-x_1+1}{2}\right) \\
&\qquad = \mathbb{I}_{x_1>y_1} f_2(x, y).
\end{aligned} \tag{3.43}
$$

**4. Asymptotics of dimers.** In this section, we will give the proofs of the results on the local asymptotics of the Aztec diamond. We start by proving Proposition 2.6 about thinned and thickened determinantal point processes.

PROOF OF PROPOSITION 2.6. Let $\{y_j\}$ be the points of the determinantal point process with kernel $K$, and let $\{n_j\}$ be independent Bernoulli random variables, $\mathbb{P}[n_j = 1] = \alpha$. Let $\mathbb{E}_K$ denote the expectation for the determinantal point process and $\mathbb{E}_n$ the expectation with respect to the Bernoulli random variables. Consider the thinned process. Then, by Fubini's theorem,

$$
\begin{aligned}
\mathbb{E}\big[e^{-\sum_j \psi(x_j)}\big] &= \mathbb{E}_n \mathbb{E}_K\big[e^{-\sum_j n_j \psi(y_j)}\big] \\
&= \mathbb{E}_K \mathbb{E}_n\Big[\prod_j \big(1 - \big(1 - e^{-n_j\psi(y_j)}\big)\big)\Big] \\
&= \mathbb{E}_K\Big[\prod_j \big(1 - \mathbb{E}_n\big[1 - e^{-n_j\psi(y_j)}\big]\big)\Big] = \mathbb{E}_K\Big[\prod_j \big(1 - \alpha\phi(y_j)\big)\Big] \qquad (4.1) \\
&= \det(I - \phi\alpha K \mathbb{I}_A), \qquad (4.2)
\end{aligned}
$$

which proves (2.22). Next, let $\{m_j\}$ be independent geometric random variables, $\mathbb{P}[m_j = k] = (1-\beta)\beta^{k-1}$, $k \geq 1$, and let $\mathbb{E}_m$ denote the expectation with respect to these random variables. Then

$$\begin{aligned}\mathbb{E}\big[e^{-\sum_j \psi(x_j)}\big] &= \mathbb{E}_m \mathbb{E}_K\big[e^{-\sum_j m_j \psi(y_j)}\big] \\ &= \mathbb{E}_K \mathbb{E}_m\bigg[\prod_j \big(1-\big(1-e^{-m_j\psi(y_j)}\big)\big)\bigg] \\ &= \mathbb{E}_K\bigg[\prod_j \bigg(1-\frac{\phi(y_j)}{1-\beta+\beta\phi(y_j)}\bigg)\bigg] \\ &= \det\bigg(I - \frac{\phi}{1-\beta+\beta\phi} K \mathbb{I}_A\bigg),\end{aligned} \tag{4.3}$$

since

$$\begin{aligned}\mathbb{E}_m\big[1-e^{-m_j\psi(y_j)}\big] &= 1-(1-\beta)\sum_{k=1}^{\infty}\beta^{k-1}e^{-k\psi(y_j)} \\ &= \frac{1-e^{-\psi(y_j)}}{1-\beta e^{-\psi(y_j)}} \\ &= \frac{\phi(y_j)}{1-\beta+\beta\phi(y_j)}.\end{aligned} \tag{4.4}$$

This proves (2.23). □

PROOF OF THEOREM 2.7. By Lemma 2.5 the south domino process on the line $y = r$ is a determinantal point process with kernel $L$ given by (2.18). Let us first consider this process in a neighbourhood of the northern boundary, when $r = [(1-k^2u(k))n]$, $k > 0$. (Below we will often neglect the integer part in this and in other expressions. It is not difficult to see that this is unimportant.) The kernel can be written

$$\begin{aligned}&L(x_1,x_2) \\ &\quad = -\frac{1}{(2\pi i)^2}\int_{\Gamma_1} dz \int_{\Gamma_2} dw\, \frac{w^{x_2-u(k)n}}{z^{x_1-u(k)n}} \frac{1}{(a+w)(w-z)} e^{ng(z)-ng(w)},\end{aligned} \tag{4.5}$$

where

$$g(z) = \big(1-k^2u(k)\big)\log(a+z) + k^2u(k)\log(az-1) - u(k)\log z. \tag{4.6}$$

We have deformed the contours $\mathcal{E}_1$ and $\mathcal{E}_2$ to new contours $\Gamma_1$ and $\Gamma_2$, described below, which are good contours for the asymptotic analysis. The argument in

the logarithms is chosen in the interval $(0, 2\pi)$. We see that when $u(k)$ is given by (2.26), $g(z)$ has a double zero at

$$z_c = \frac{1}{a + k\sqrt{1+a^2}}. \tag{4.7}$$

We can now use a saddle-point argument to analyze the relevant asymptotics of (4.5), and since this is a fairly standard Airy kernel asymptotics saddle point analysis, we will not go into all the details. For the integration contours in (4.5) we have chosen the steepest descent contours given by the level lines of the imaginary part of $g(z)$ starting at $z_c$. It can be seen that we will have two ascending contours for the real part of $g(z)$ which will leave in the directions $e^{\pm\pi i/3}$ and go to infinity. We can deform the contour $\mathcal{E}_2$ to a contour $\Gamma_2$ consisting of these two pieces. We will have two descending contours going from $z_c$ to $-a$ leaving in the directions $e^{\pm 2\pi i/3}$, and these can be combined into a contour $\Gamma_1$; see Figure 7. If we have the scalings

$$x_1 = \big[u(k)n - \lambda n^{1/3}\xi\big], \qquad x_2 = \big[u(k)n - \lambda n^{1/3}\eta\big], \tag{4.8}$$

then

$$\begin{aligned} &\lim_{n\to\infty} -\lambda n^{1/3} z_c^{x_1-x_2} L(x_1, x_2) \\ &\quad = \alpha \frac{1}{(2\pi i)^2} \int_\Gamma dz \int_\Gamma dw\, \frac{1}{i(z+w)} e^{iz^3/3 + i\xi z + iw^3/3 + i\eta w} \end{aligned} \tag{4.9}$$

$$= \alpha K_{\mathrm{Ai}}(\xi, \eta) \tag{4.10}$$

uniformly for $\xi, \eta$ in a compact subset of $\mathbb{R}$, where $\alpha = z_c/(z_c + a)$. Here $\Gamma$ is given by $z(t) = -te^{(\pi-\theta)i}$, $t < 0$ and $z(t) = te^{i\theta}$, $t \geq 0$, with a fixed $0 < \theta < \pi/3$.

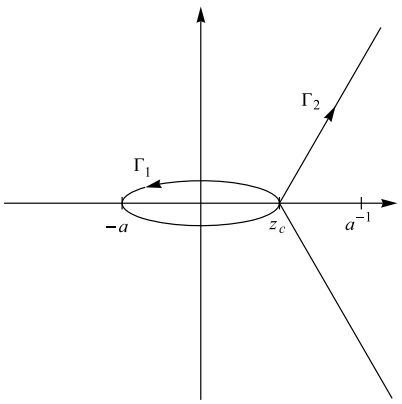


FIG. 7. *A schematic diagram of the contours of steepest ascent and descent for $g(z)$ for $z_c \in (0, 1/a)$.*

Furthermore, $\lambda$ is given by

$$\lambda = z_c\bigl(-g^{(3)}(z_c)/2\bigr)^{1/3}. \tag{4.11}$$

A computation gives (2.30). To prove the result in Theorem 2.7 we observe that, with $\phi = 1 - e^{-\psi}$ and $[n] = \{1, \dots, n\}$,

$$\begin{aligned}&\mathbb{E}\bigl[e^{-\sum_j \psi(\xi_j)}\bigr]\\ &\quad= \mathbb{E}\biggl[\prod_j \biggl(1 - \phi\biggl(\frac{nu(k) - x_j}{\lambda n^{1/3}}\biggr)\biggr)\biggr]\end{aligned} \tag{4.12}$$

$$= \sum_{m=0}^{n} \frac{(-1)^m}{m!} \sum_{x_1,\dots,x_m \in [n]} \prod_{j=1}^{m} \phi\biggl(\frac{nu(k) - x_j}{\lambda n^{1/3}}\biggr) \det\bigl(L(x_i, x_j)\bigr)_{m\times m}. \tag{4.13}$$

Using the uniform convergence in (4.9) and Hadamard's inequality, we see that (4.12) converges to

$$\begin{aligned}&\sum_{m=0}^{n} \frac{(-1)^m}{m!} \int_{\mathbb{R}^m} \prod_{j=1}^{m} \phi(\xi_j) \det\bigl(\alpha K_{\mathrm{Ai}}(\xi_i, \xi_j)\bigr)_{m\times m} d^m\xi\\ &\quad= \det(I - \phi\alpha K_{\mathrm{Ai}}\mathbb{I}_A),\end{aligned} \tag{4.14}$$

for every $\psi \in C_c^+(\mathbb{R})$, where $A = \operatorname{supp}\phi = \operatorname{supp}\psi$; see, for example, [22]. This proves the weak convergence claimed in the theorem; see, for example, [11], page 138.

We turn now to the south domino process close to the southern boundary. Take $r$ as before but with $k \in (-a^{-1}(1+a^2)^{1/2}, -a(1+a^2)^{-1/2})$. By Lemma 2.5

$$L(x_1, x_2) = -\frac{1}{(2\pi i)^2} \int_{\mathcal{E}_1} dz \int_{\mathcal{E}_2} dw\, \frac{w^{x_2}}{z^{x_1}} \frac{(a+z)^r (az-1)^{n-r}}{(a+w)^{r+1}(aw-1)^{n-r}} \frac{1}{w-z}. \tag{4.15}$$

Deform $\mathcal{E}_2$ through infinity to a contour $\gamma_2$ containing $\mathcal{E}_1$ and $-a$ in its interior, but $1/a$ outside, to obtain

$$L(x_1, x_2) = \frac{1}{(2\pi i)^2} \int_{\mathcal{E}_1} dz \int_{\gamma_2} dw\, \frac{w^{x_2}}{z^{x_1}} \frac{(a+z)^r (az-1)^{n-r}}{(a+w)^{r+1}(aw-1)^{n-r}} \frac{1}{w-z}. \tag{4.16}$$

Then move $\mathcal{E}_1$ to a contour $\gamma_1$ which surrounds $\gamma_2$; see Figure 8. This picks up a contribution from the pole at $z = w$. Write

$$\widetilde{L}(x_1, x_2) = \frac{z_c^{x_1 - x_2}}{(2\pi i)^2} \int_{\gamma_1} dz \int_{\gamma_2} dw\, \frac{w^{x_2}}{z^{x_1}} \frac{(a+z)^r (az-1)^{n-r}}{(a+w)^{r+1}(aw-1)^{n-r}} \frac{1}{w-z}. \tag{4.17}$$

Here $z_c$ is again given by (4.7). Note that now we have $z_c \in (-\infty, -a)$. Thus we find

$$z_c^{x_1 - x_2} L(x_1, x_2) = \frac{z_c^{x_1 - x_2}}{2\pi i} \int_{\gamma_1} \frac{z^{x_2 - x_1}}{z+a}\, dz + \widetilde{L}(x_1, x_2). \tag{4.18}$$

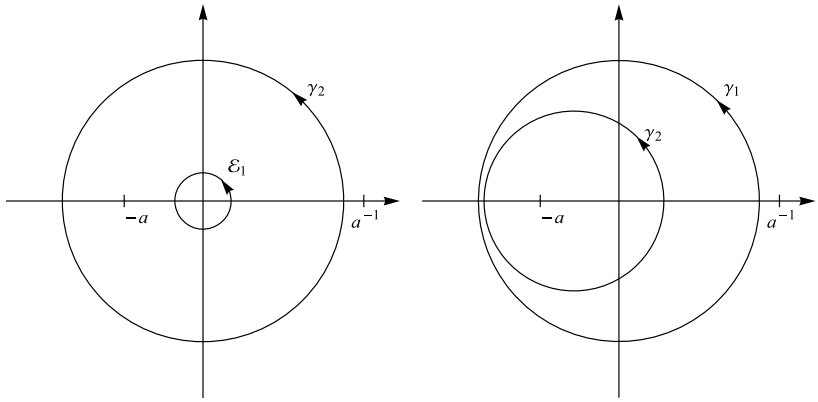


FIG. 8. *The figure on the left represents deforming the contour $\mathcal{E}_2$ to $\gamma_2$. The figure on the right represents deforming the contour $\mathcal{E}_1$ through $\gamma_2$ to $\gamma_1$. Note that this picks up a single integral term.*

The parameter $\beta$ of the thickened process is given by $\beta = -a/z_c$, and we see that $0 < \beta < 1$. Set

$$M(x_1, x_2) = -\beta^{x_2 - x_1} \mathbb{I}_{x_1 < x_2}. \tag{4.19}$$

Then (4.18) gives

$$z_c^{x_1 - x_2} L(x_1, x_2) = \delta_{x_1, x_2} - M(x_1, x_2) + \widetilde{L}(x_1, x_2). \tag{4.20}$$

A correlation kernel $L^*$ for the dual point process is given by [2], Proposition 4,

$$L^*(x_1, x_2) = \delta_{x_1, x_2} - z_c^{x_1 - x_2} L(x_1, x_2) = M(x_1, x_2) - \widetilde{L}(x_1, x_2). \tag{4.21}$$

If $x_1, x_2, \ldots$ are the points in the dual point process, we want to look at

$$\mathbb{E}\Big[\prod_j \exp\Big(-\sum_j \psi\Big(\frac{x_j - nu(k)}{\lambda n^{1/3}}\Big)\Big)\Big] = \det\big(I - fL^* g\big), \tag{4.22}$$

where the Fredholm determinant is on $\ell^2(\{1, \ldots, n\})$ and so is actually a determinant of a finite matrix. Here we have introduced $f(x) = \phi((\lambda n^{1/3})^{-1}(x - u(k)n))$ and $g(x) = \mathbb{I}_A((\lambda n^{1/3})^{-1}(x - u(k)n))$, where $A$ is the support of $\phi$. Now, by (4.21), we have

$$\det\big(I - fL^* g\big) = \det(I - fMg + f\widetilde{L}g) \tag{4.23}$$

$$\begin{aligned} &= \det(I - fMg)\det\big(I + (I - fMg)^{-1} f\widetilde{L}\big) \\ &= \det\Big(I + \sum_{j=0}^{n} (fMg)^j f\widetilde{L}g\Big) \end{aligned} \tag{4.24}$$

$$= \det\Big(I + f\sum_{j=0}^{n} (Mf)^j \widetilde{L}g\Big). \tag{4.25}$$

Here we have used that $gf = f$ and $fMg$ is nilpotent, $(fMg)^{n+1} = 0$. Hence, we also have $\det(I - fMg) = 1$. Set

$$R = \sum_{j=1}^{n} (Mf)^j \widetilde{L}. \tag{4.26}$$

Then, by (4.23), we have

$$\det(I - fL^*g) = \det(I + f(R + \widetilde{L})g). \tag{4.27}$$

In order to prove the result in Theorem 2.7 it suffices to show that, with the scaling

$$x_1 = [u(k)n + \lambda n^{1/3}\xi], \qquad x_2 = [u(k)n + \lambda n^{1/3}\eta] \tag{4.28}$$

we have that

$$\lambda n^{1/3}(R + \widetilde{L})(x_1, x_2) \to -\frac{1}{1 - \beta + \beta\phi(\xi)} K_{\mathrm{Ai}}(\xi, \eta) \tag{4.29}$$

uniformly for $\xi, \eta$ in a compact subset of $\mathbb{R}$ as $n \to \infty$. We will prove this under the assumption that $\psi$ is also continuously differentiable, which suffices to show the weak convergence of the point process. This can be seen by an approximation argument.

We will make use of the following fact given below in (4.30), which again is proved by a saddle point argument very similar to the one discussed above. The only difference is in the choice of contours. As integration contours we will again choose level lines of the imaginary part of $g(z)$ starting at $z_c$. Recall that $z_c \in (-\infty, -a)$. It can be seen that we will have two ascending contours for the real part of $g(z)$ which will leave in the directions $e^{\pm\pi i/3}$ and go to 0. We combine these contours to a contour $\gamma_2'$ and use it for our $w$-integration. We will have two descending contours going from $z_c$ to $1/a$ leaving in the directions $e^{\pm 2\pi i/3}$. Combine them into a contour $\gamma_1'$, and use it for the $z$-integration.

Let $x_1, x_2$ be as in (4.28), $r = [(1 - k^2 u(k))n]$ and $k \in (-a(1 + a^2)^{-1/2}, -a^{-1}(1 + a^2)^{1/2})$. Then, we have

$$\begin{aligned} &\frac{\lambda n^{1/3} z_c^{x_1 - x_2}}{(2\pi i)^2} \int_{\gamma_1'} dz \int_{\gamma_2'} dw\, F(z) \frac{w^{x_2}}{z^{x_1}} \frac{(a + z)^r (az - 1)^{n-r}}{(a + w)^{r+1}(aw - 1)^{n-r}} \frac{1}{w - z} \\ &\qquad \to -\frac{D}{1 - \beta} K_{\mathrm{Ai}}(\xi, \eta) \end{aligned} \tag{4.30}$$

uniformly for $\xi, \eta$ in compacts as $n \to \infty$, for $F(z) = 1$ or $F(z) = \beta z_c f(x_1)/(z - \beta(1 - f(x_1))z_c)$, where $D = F(z_c)$. Note that with the scaling (4.28) we have $f(x_1) = \phi(\xi)$ (ignoring integer parts).

By expanding $M$ and rearranging the sum, we have

$$\begin{aligned}
&R(x_1,x_2)\\
&\quad=\sum_{j=1}^{n}(Mf)^j\widetilde{L}(x_1,x_2)\\
&\quad=\sum_{j=1}^{n}(-1)^j\sum_{y_1,\dots,y_j\in[n]}\beta^{y_j-x_1}\mathbb{I}_{(x_1<y_1)}\cdots\mathbb{I}_{(y_{j-1}<y_j)}f(y_1)\cdots f(y_j)\widetilde{L}(y_j,x_2)\\
&\quad=\sum_{j=1}^{n}(-1)^j\sum_{t=j}^{n-x_1}\beta^t f(x_1+t)\widetilde{L}(x_1+t,x_2)\\
&\qquad\times\sum_{x_1<y_1<\cdots<y_{j-1},x_1+t}f(y_1)\cdots f(y_{j-1}).
\end{aligned}$$

Let $e_j(x_1,\dots,x_{t-1})$ be the $j$th elementary symmetric polynomial in $t-1$ variables, and write $f=(f(x_1+1),\dots,f(x_1+t-1))$. By interchanging the sums, we obtain

$$\begin{aligned}
R(x_1,x_2)&=-\sum_{t=1}^{n-x_1}\beta^t f(x_1+t)\widetilde{L}(x_1+t,x_2)\sum_{j=0}^{t-1}(-1)^{j-1}e_{j-1}(f)\\
&=-\sum_{t=1}^{n-x_1}\beta^t f(x_1+t)\widetilde{L}(x_1+t,x_2)\prod_{j=1}^{t-1}\bigl(1-f(x_1+j)\bigr).
\end{aligned}\tag{4.31}$$

Set

$$T(x_1,x_2)=-\sum_{t=1}^{n-x_1}\beta^t f(x_1)\bigl(1-f(x_1)\bigr)^{t-1}\widetilde{L}(x_1+t,x_2).\tag{4.32}$$

We then have the following:

CLAIM 1. *For all $\xi,\eta$ in a compact subset of $\mathbb{R}$ there is a constant $C$ such that if we have the scaling* (4.28), *then*

$$\bigl|\lambda n^{1/3}(R-T)(x_1,x_2)\bigr|\le\frac{C}{n^{1/3}}.\tag{4.33}$$

We proceed with the proof of the theorem and return to the proof of the claim below. Using (4.17) we see that

$$\begin{aligned}
T(x_1,x_2)&=-\sum_{t=1}^{n-x_1}\beta^t f(x_1)\bigl(1-f(x_1)\bigr)^{t-1}\frac{z_c^{x_1-x_2}}{(2\pi i)^2}\\
&\quad\times\int_{\gamma_1}dz\int_{\gamma_2}dw\left(\frac{z_c}{z}\right)^t\frac{w^{x_2}}{z^{x_1}}\frac{(a+z)^r(az-1)^{n-r}}{(a+w)^{r+1}(aw-1)^{n-r}}\frac{1}{w-z}
\end{aligned}\tag{4.34}$$

$$
\begin{aligned}
&= -\frac{f(x_1)}{1-f(x_1)}\frac{z_c^{x_1-x_2}}{(2\pi i)^2} \\
&\quad \times \int_{\gamma_1} dz \int_{\gamma_2} dw\, \frac{\beta(1-f(x_1))z_c/z - (\beta(1-f(x_1))z_c/z)^{n-x_1+1}}{1-\beta(1-f(x_1))z_c/z} \\
&\qquad \times \frac{w^{x_2}}{z^{x_1}} \frac{(a+z)^r (az-1)^{n-r}}{(a+w)^{r+1}(aw-1)^{n-r}} \frac{1}{w-z} \\
&= -f(x_1)\frac{z_c^{x_1-x_2}}{(2\pi i)^2} \int_{\gamma_1} dz \int_{\gamma_2} dw\, \frac{\beta z_c}{z-\beta(1-f(x_1))z_c} \frac{w^{x_2}}{z^{x_1}} \\
&\qquad \times \frac{(a+z)^r (az-1)^{n-r}}{(a+w)^{r+1}(aw-1)^{n-r}} \frac{1}{w-z}.
\end{aligned}
$$

The term involving $(\beta(1-f(x_1))z_c/z)^{n-x_1+1}$ does not contribute since the $z$-integral integrates to 0 by Cauchy's theorem because the integrand is analytic outside $\gamma_1$ including at $\infty$.

It now follows from (4.30) that

$$
\lambda n^{1/3} T(x_1, x_2) \to \frac{\beta\phi(\xi)}{1-\beta(1-\phi(\xi))} \frac{1}{1-\beta} K_{\mathrm{Ai}}(\xi, \eta) \tag{4.35}
$$

uniformly as $n \to \infty$. If we combine this with (4.33) and the fact, again by (4.30) with $F(z) = 1$, that

$$
\lambda n^{1/3} \widetilde{L}(x_1, x_2) \to -\frac{1}{1-\beta} K_{\mathrm{Ai}}(\xi, \eta) \tag{4.36}
$$

we obtain (4.29), which is what we wanted to prove.

It remains to prove the claim. We will use the following two facts. If $\xi, \eta$ belongs to a compact subset, there is a constant $B > 0$ and a constant $C$ such that if we have the scaling (4.8), then: (i) $f(x_1 + t) = 0$ if $t \notin [-Bn^{1/3}, Bn^{1/3}]$ and (ii) $|\lambda n^{1/3} \widetilde{L}(x_1 + t, x_2)| \le C$ for all $t \in [-Bn^{1/3}, Bn^{1/3}]$. That (i) holds follows immediately from the fact that $\phi$ has compact support, and (ii) follows from (4.30) in the case $F(z) = 1$ since we have uniform convergence. We will also use the inequality

$$
\left| \prod_{j=1}^{n} a_j - \prod_{j=1}^{n} b_j \right| \le \sum_{j=1}^{n} |a_j - b_j|,
$$

provided $|a_j|, |b_j| \le 1$ for all $j$. This is easy to prove by induction.

Now, since $\phi$ is continuously differentiable and has compact support,

$$\begin{aligned}
&\left| f(x_1+t)\prod_{j=1}^{t-1}\bigl(1-f(x_1+j)\bigr) - f(x_1)\prod_{j=1}^{t-1}\bigl(1-f(x_1)\bigr)\right| \\
&\quad\le \sum_{j=1}^{t}\bigl|f(x_1+j)-f(x_1)\bigr| \\
&\quad= \sum_{j=1}^{t}\left|\phi\Bigl(\frac{[u(k)n+\lambda n^{1/3}\xi]+j-u(k)n}{\lambda n^{1/3}}\Bigr)\right. \\
&\qquad\qquad \left. -\,\phi\Bigl(\frac{[u(k)n+\lambda n^{1/3}\xi]-u(k)n}{\lambda n^{1/3}}\Bigr)\right| \\
&\quad\le \sum_{j=1}^{t}\frac{Cj}{n^{1/3}} \le \frac{Ct^2}{n^{1/3}},
\end{aligned} \tag{4.37}$$

for some constant $C$. Thus

$$\begin{aligned}
&\bigl|\lambda n^{1/3}(R-T)(x_1,x_2)\bigr| \\
&\quad\le \sum_{t=1}^{n-x_1}\beta^t\bigl|f(x_1+t)\bigr|\bigl|\lambda n^{1/3}\widetilde{L}(x_1+t,x_2)\bigr| \\
&\qquad\times\left| f(x_1+t)\prod_{j=1}^{t-1}\bigl(1-f(x_1+t)\bigr) - f(x_1)\prod_{j=1}^{t-1}\bigl(1-f(x_1)\bigr)\right| \\
&\quad\le \frac{C}{n^{1/3}}\sum_{t=1}^{n-x_1}\beta^t t^2 \le \frac{C}{n^{1/3}},
\end{aligned} \tag{4.38}$$

since $0<\beta<1$. In the next to last inequality we used (i) and (ii) above. The estimate (ii) works since we can use (i) to restrict the range of $t$-values. □

Above we have been concerned with the behavior of the south dominoes at the boundary of the frozen region. We can also consider the behavior of the south dominoes as we enter the bulk but still stay close to the boundary at a macroscopic scale. We then get as a scaling limit the thinned sine kernel point process with the same parameter $\alpha$. We will not go into the details.

Next we will give the proof of Theorem 2.8 which is concerned with the case when $a$ grows with $n$ but not too fast. In the case when $a$ instead goes to zero with $n$ but not to fast we should have convergence to the Airy kernel point process at the northern boundary for the south domino process. Note that the thinning parameter $\alpha\to 1$ as $a\to 0$. If $a=\gamma/n$ for some fixed $\gamma>0$, then we expect instead the

discrete Bessel kernel in the limit as $n \to \infty$. We will not go into the details on how to prove these assertions.

PROOF OF THEOREM 2.8. Set

$$\mathcal{L}(x_1, x_2) = z_c^{x_1 - x_2} L(x_1, x_2), \tag{4.39}$$

with $L$ as in (4.5) and $z_c$ given by (4.7). Take $\phi \in C_c(\mathbb{R})$, $0 \le \phi \le 1$, and let

$$f(j) = \phi\left(\frac{nu(k) + c(a)n^{1/3} - j}{c(a)n^{1/3}}\right) \tag{4.40}$$

for $j \in \mathbb{Z}$. Furthermore, define

$$\begin{aligned} M_n(\xi, \eta) = -c(a)n^{1/3} \mathcal{L}\big(&\big[u(k)n - c(a)n^{1/3}(\xi - 1)\big], \\ &\big[u(k)n - c(a)n^{1/3}(\eta - 1)\big]\big). \end{aligned} \tag{4.41}$$

Set

$$I_j = \left(\frac{u(k)n + c(a)n^{1/3} - (j+1)}{c(a)n^{1/3}}, \frac{u(k)n + c(a)n^{1/3} - j}{c(a)n^{1/3}}\right], \tag{4.42}$$

for $j \in \mathbb{Z}$, and for $\xi \in I_j$, define $\tilde{\phi}_n(\xi) = f(j)$.

Let $A$ be a compact subset of the real line such that $\operatorname{supp} \tilde{\phi}_n \subseteq A$ for all $n$. Then

$$\begin{aligned} &\mathbb{E}\left[\prod_j (1 - \phi(\xi_j))\right] \\ &\quad = \sum_{m=0}^{n} \frac{(-1)^m}{m!} \sum_{x_1, \dots, x_m \in [n]} \prod_{j=1}^{m} f(x_j) \det\big(\mathcal{L}(x_i, x_j)\big)_{m \times m} \end{aligned} \tag{4.43}$$

$$= \sum_{m=0}^{n} \frac{(-1)^m}{m!} \int_{\mathbb{R}^m} \prod_{j=1}^{m} \tilde{\phi}_n(\xi_j) \det\big(M_n(\xi_i, \xi_j)\big)_{m \times m} d^m \xi \tag{4.44}$$

$$= \det(I - \tilde{\phi}_n M_n \mathbb{I}_A)_{L^2(\mathbb{R})}, \tag{4.45}$$

where $[n] = \{1, \dots, n\}$. The second equality follows from (4.39) to (4.42) and the fact that the integrand is constant on the intervals $I_j$ in each variable. Assume that we can show that

$$\|\tilde{\phi}_n M_n \mathbb{I}_A\|_2 \to 0 \tag{4.46}$$

as $n \to \infty$, where $\|\cdot\|_2$ is the Hilbert–Schmidt norm, and

$$M_n(\xi, \xi) \to \sqrt{(1 - \xi)_+} \tag{4.47}$$

uniformly for $\xi \in A$ as $n \to \infty$. The result then follows from (4.43) in the following way. If the operators $B_n$ on $L^2(\mathbb{R})$ are trace class then the determinant $\det_2(I + B_n)$ and the Fredholm determinant $\det(I + B_n)$ are related by

$$\det(I + B_n) = e^{\operatorname{tr} B_n} \det_2(I + B_n). \tag{4.48}$$

Also, if we have $\|B_n\|_2 \to 0$ as $n \to \infty$, then we have $\det_2(I + B_n) \to 1$ as $n \to \infty$; see [18]. Hence

$$\det(I - \tilde{\phi}_n M_n \mathbb{I}_A) = e^{\operatorname{tr} \tilde{\phi}_n M_n \mathbb{I}_A} \det_2(I - \tilde{\phi}_n M_n \mathbb{I}_A). \tag{4.49}$$

It follows from (4.46) that $\det_2(I - \tilde{\phi}_n M_n 1_A) \to 0$ as $n \to \infty$, and from (4.47) that

$$\operatorname{tr} \tilde{\phi}_n M_n 1_A = \int_{\mathbb{R}} \tilde{\phi}_n(\xi) M_n(\xi, \xi)\, d\xi \to \int_{\mathbb{R}} \phi(\xi) \sqrt{(1-\xi)_+}\, d\xi, \tag{4.50}$$

as $n \to \infty$. Thus, by (4.43) and (4.49),

$$\lim_{n\to\infty} \mathbb{E}\Big[\prod_j (1 - \phi(\xi_j))\Big] = e^{-\int_{\mathbb{R}} \phi(\xi)\sqrt{(1-\xi)_+}\, d\xi}, \tag{4.51}$$

which is what we wanted to prove.

We turn now to the asymptotic analysis of $M_n$ and the proof of (4.46) and (4.47). We will denote by $C$ a generic constant that can depend on $k$ and $d$ in Claim 2 but not on $n$ or $a$. Let $\lambda$ be given by (2.30) and define

$$M_n^{(1)}(\xi, \eta) = -\lambda n^{1/3} \mathcal{L}\big([nu(k) - \lambda n^{1/3}\xi], [nu(k) - \lambda n^{1/3}\eta]\big). \tag{4.52}$$

CLAIM 2. *Let $\alpha$ be given by (2.29) and fix $d > 0$. Then*

$$\big|M_n^{(1)}(\xi, \eta) - \alpha K_{\mathrm{Ai}}(\xi, \eta)\big| \le \frac{C}{a^2} \tag{4.53}$$

*for all $\xi, \eta \in [-da^{4/3}, da^{4/3}]$.*

Before proving the claim we finish the proof of the theorem. Set $\tilde{c}(a) = c(a)/\lambda$, and note that $\tilde{c}(a) \sim \pi^{2/3} a^{4/3} (1+k)^{2/3}$ as $a \to \infty$. Then we find that

$$M_n(\xi + 1, \eta + 1) = \tilde{c}(a) M_n^{(1)}\big(\tilde{c}(a)\xi, \tilde{c}(a)\eta\big). \tag{4.54}$$

Thus, with an appropriate fixed $d_1 > 0$, we have

$$\begin{aligned} \|\tilde{\phi}_n M_n \mathbb{I}_A\|_2 &= \int_{\mathbb{R}^2} \tilde{\phi}_n(x)^2 M_n(x, y)^2 \mathbb{I}_A(y)\, dx\, dy \\ &\le \int_{[-d_1, d_1]^2} M_n(\xi + 1, \eta + 1)^2\, d\xi\, d\eta \\ &= \tilde{c}(a)^2 \int_{[-d_1, d_1]^2} M_n^{(1)}\big(\tilde{c}(a)\xi, \tilde{c}(a)\eta\big)^2\, d\xi\, d\eta \\ &= \int_{[-da^{4/3}, da^{4/3}]^2} M_n^{(1)}(\xi, \eta)^2\, d\xi\, d\eta, \end{aligned} \tag{4.55}$$

where $d = d_1\pi^{2/3}(1+k)^{2/3}$. Using (4.53) we see that

$$\|\tilde{\phi}_n M_n \mathbb{I}_A\|_2 \le 2\alpha^2 \int_{[-da^{4/3},da^{4/3}]^2} K_{\mathrm{Ai}}(\xi,\eta)^2\,d\xi\,d\eta + Cd^2\big(a^{4/3}a^{-2}\big)^2. \tag{4.56}$$

Now $a^{-4/3} \to 0$, since $a = a(n) \to \infty$ as $n \to \infty$, and we see that in order to prove (4.46) it remains to control the integral in (4.56). If we use the identities

$$\int_{-\infty}^{\infty} K_{\mathrm{Ai}}(x,y)^2\,dy = K_{\mathrm{Ai}}(x,x), \tag{4.57}$$

and

$$K_{\mathrm{Ai}}(x,x) = \mathrm{Ai}'(x)^2 - x\,\mathrm{Ai}(x)^2 \tag{4.58}$$

we see that

$$\begin{aligned}
&2\alpha^2 \int_{[-da^{4/3},da^{4/3}]^2} K_{\mathrm{Ai}}(\xi,\eta)^2\,d\xi\,d\eta \\
&\quad\le 2\alpha^2 \int_{-da^{4/3}}^{\infty}\left(\int_{-\infty}^{\infty} K_{\mathrm{Ai}}(\xi,\eta)^2\,d\eta\right)d\xi \\
&\quad= 2\alpha^2 \int_{-da^{4/3}}^{\infty} K_{\mathrm{Ai}}(\xi,\xi)\,d\xi = 2\alpha^2 \int_{-da^{4/3}}^{\infty} \mathrm{Ai}'(\xi)^2 - \xi\,\mathrm{Ai}(\xi)^2\,d\xi \\
&\quad= \frac{2\alpha^2}{3}\big[2\big(da^{4/3}\big)^2\,\mathrm{Ai}^2\big(-da^{4/3}\big) \\
&\qquad\quad + 2da^{4/3}\,\mathrm{Ai}'\big(-da^{4/3}\big)^2 - \mathrm{Ai}\big(-da^{4/3}\big)\,\mathrm{Ai}'\big(-da^{4/3}\big)\big].
\end{aligned} \tag{4.59}$$

Now, as $r \to \infty$ we have

$$\begin{aligned}
\mathrm{Ai}(-r) &= \frac{1}{\sqrt{\pi}} r^{-1/4} \sin\left(\frac{2}{3}r^{3/2} + \frac{\pi}{4}\right) + \cdots, \\
\mathrm{Ai}'(-r) &= \frac{1}{\sqrt{\pi}} r^{1/4} \cos\left(\frac{2}{3}r^{3/2} + \frac{\pi}{4}\right) + \cdots
\end{aligned} \tag{4.60}$$

and hence, since $\alpha \sim (1+k)^{-1}a^{-2}$ for large $a$, we obtain the bound

$$2\alpha^2 \int_{[-da^{4/3},da^{4/3}]^2} K_{\mathrm{Ai}}(\xi,\eta)^2\,d\xi\,d\eta \le Ca^{-4}\big(da^{4/3}\big)^{3/2} \le Ca^{-2}, \tag{4.61}$$

and since $a = a(n) \to \infty$ we have proved (4.46).

We now turn to the proof of (4.47). It follows from (4.53) and (4.54) that

$$\begin{aligned}
\big|M_n(\xi,\xi) - \alpha\tilde{c}(a)K_{\mathrm{Ai}}\big(\tilde{c}(a)(\xi-1),\tilde{c}(a)(\xi-1)\big)\big| &\le Ca^{4/3}a^{-2} \\
&= Ca^{-2/3}
\end{aligned} \tag{4.62}$$

for all $\xi$ in a compact interval, and since $a \to \infty$ as $n \to \infty$, (4.47) follows by using (4.58) and standard asymptotic formulas for the Airy function and its derivative.

It remains to prove Claim 2. Let $\gamma > 0$ be given by $\gamma^3 g^{(3)}(z_c) = -2$. From (4.11) we see that that $\lambda = z_c/\gamma$. Let $g(z)$ be defined by (4.6) and write

$$f_\xi(\zeta) = \lambda n^{1/3}\xi \log\left(1 + \frac{\gamma\zeta}{z_c n^{1/3}}\right) \tag{4.63}$$

and

$$F_\xi(\zeta) = f_\xi(\zeta) + n\big(g\big(z_c + \gamma\zeta n^{-1/3}\big) - g(z_c)\big). \tag{4.64}$$

If we use (4.5) and make the change of variables $z = z_c + \gamma\zeta n^{-1/3}$, $w = z_c + \gamma\omega n^{-1/3}$ we obtain

$$M_n^{(1)}(\xi,\eta) = \frac{\alpha}{(2\pi i)^2}\int_{\mathcal{C}} d\zeta \int_{\mathcal{D}} d\omega \, \frac{a + z_c}{(a + z_c + \gamma\omega n^{-1/3})(\omega - \zeta)} \times e^{F_\xi(\zeta) - F_\eta(\omega)}, \tag{4.65}$$

where $\mathcal{C}$ and $\mathcal{D}$ are the images of the steepest descent contours in Theorem 2.7. If $|\omega| \geq a^2 n^{1/3}$ we have the estimate

$$\big|e^{-F_\eta(\omega)}\big| \leq C^n a^{2n}\left|\frac{n^{1/3}}{a^{2/3}\omega}\right|^{n/2} \tag{4.66}$$

for all sufficiently large $n$. $\mathcal{C}$ will lie inside $|\zeta| \leq a^2 n^{1/3}$, and using (4.66) and the estimates we describe below for the $\zeta$-integration, we see that we can replace $\mathcal{D}$ by the part of $\mathcal{D}$ that lies inside $|\omega| \leq a^2 n^{1/3}$. We denote this part by $\mathcal{D}$ also for simplicity.

Let $\mathcal{C}_1^*$ be the part of $\mathcal{C}$ in the disk $|\zeta| \leq n^{1/15}$, $\mathcal{C}_2^*$ the part in the annulus $n^{1/15} \leq |\zeta| \leq n^{7/45}$ and $\mathcal{C}_3^*$ the part in $|\zeta| \geq n^{7/45}$. Let $\mathcal{C}_i$ and $\overline{\mathcal{C}_i}$ be the parts of $\mathcal{C}_i^*$ that lie in the upper and lower half plane, respectively. We make the analogous definitions for $\mathcal{D}$. We will consider estimates of $F_\xi(\zeta)$ on $\mathcal{C}_i$, $i = 1, 2, 3$. The estimates on $\overline{\mathcal{C}_i}$ are the same by symmetry, and the estimates on $\mathcal{D}$ are analogous. The estimates that we need are

$$\operatorname{Re} n\big(g\big(z_c + \gamma\zeta n^{-1/3}\big) - g(z_c)\big) \leq -\tfrac{1}{6}|\zeta|^3 \tag{4.67}$$

for all $\zeta \in \mathcal{C}_1 + \mathcal{C}_2$ and

$$\operatorname{Re} n\big(g\big(z_c + \gamma\zeta n^{-1/3}\big) - g(z_c)\big) \leq -\tfrac{1}{6}n^{7/15} \tag{4.68}$$

for all $\zeta \in \mathcal{C}_3$ and $n$ sufficiently large. To see this note that we can write

$$n\big(g\big(z_c + \gamma\zeta n^{-1/3}\big) - g(z_c)\big) = -\tfrac{1}{3}\zeta^3 + h_1(\zeta), \tag{4.69}$$

where

$$h_1(\zeta) = \frac{\gamma^4}{6n^{1/3}}\int_0^\zeta g^{(4)}\left(z_c + \frac{\gamma s}{n^{1/3}}\right)(\zeta - s)^3\, ds. \tag{4.70}$$

Now, if we have $|\zeta| \le n^{7/45}$, then

$$|h_1(\zeta)| \le Ca^{2/3}n^{-1/3}|\zeta|^4. \tag{4.71}$$

The estimate (4.71) follows from the fact that

$$\left|g^{(4)}\left(z_c + \frac{\gamma s}{n^{1/3}}\right)\right| \le Ca^2 \tag{4.72}$$

for $|s| \le n^{7/45}$ since $\gamma \le Ca^{-1/3}$. If we have $\zeta \in \mathcal{C}_1 + \mathcal{C}_2$, then $0 = -\frac{1}{3}\operatorname{Im}\zeta^3 + \operatorname{Im}h_1(\zeta)$, and if we write $\zeta = re^{i\theta}$, this gives $r^3 \sin 3\theta = 3\operatorname{Im}h_1(re^{i\theta})$ and hence, by (4.71),

$$|\sin 3\theta| \le Ca^{2/3}n^{-1/3}r \le Cn^{-1/9}. \tag{4.73}$$

Since $\mathcal{C}_1$ leaves $z_c$ in the direction $e^{2\pi i/3}$, we must have $\cos 3\theta \ge 2/3$ for all large $n$. Thus

$$\begin{aligned} &\operatorname{Re} n\big(g\big(z_c + \gamma\zeta n^{-1/3}\big) - g(z_c)\big) \\ &\quad = -\tfrac{1}{3}|\zeta|^3 \cos 3\theta + \operatorname{Re}h_1(\zeta) \end{aligned} \tag{4.74}$$

$$\le -\tfrac{2}{9}|\zeta|^3\big(1 - Ca^{2/3}n^{-1/3}|\zeta|\big) \le -\tfrac{1}{6}|\zeta|^3 \tag{4.75}$$

if $\zeta \in \mathcal{C}_1 + \mathcal{C}_2$ and $n$ is large. This proves (4.67). Since $\operatorname{Re} n(g(z_c + \gamma\zeta n^{-1/3}) - g(z_c))$ is decreasing as we move along $\mathcal{C}$ in the upper half plane starting at $z_c$, we see that the value on $\mathcal{C}_3$ must be $\le -n^{7/15}/6$ by using the estimate (4.67) at the point where $\mathcal{C}$ meets $|\zeta| = n^{7/15}$ (the endpoint of $\mathcal{C}_2$). This proves (4.68).

We can write

$$f_\xi(\zeta) = \xi\zeta + \xi h_2(\zeta), \tag{4.76}$$

where

$$h_2(\zeta) = -\frac{1}{\lambda n^{1/3}}\int_0^\zeta \frac{\zeta - s}{(1 + s/\lambda n^{1/3})^2}\,ds, \tag{4.77}$$

and we see that if $|\zeta| \le n^{7/45}$, then

$$|h_2(\zeta)| \le Ca^{2/3}n^{-1/3}|\zeta|^2. \tag{4.78}$$

We start by estimating $F_\xi(\zeta)$ on $\mathcal{C}_3$. If $\zeta \in \mathcal{C}_3$, then $|\zeta| \le a^2 n^{1/3}$ and hence

$$\operatorname{Re} f_\xi(\zeta) = \lambda\xi n^{1/3}\log\left|1 + \frac{\zeta}{\lambda n^{1/3}}\right| \le Cn^{6/15}\log n, \tag{4.79}$$

and combining this with (4.68), we see that $\operatorname{Re}F_\xi(\zeta) \le -\frac{1}{12}n^{7/15}$ for large $n$, and hence the contribution from $\mathcal{C}_3$ is negligible.

Since $|\xi| \le Ca^{4/3}$ and $a \le Cn^{1/10}$ we see that if $\zeta \in \mathcal{C}_2$, then $\operatorname{Re}f_\xi(\zeta) \le Cn^{1/10}|\zeta|$. Combining this with (4.67) we see that $\operatorname{Re}F_\xi(\zeta) \le -|\zeta|^3/12$ for $n$ large, and hence the contribution from $\mathcal{C}_2$ is negligible.

Thus, with an error that is much smaller than $Ca^{-2}$, we can replace $M_n^{(1)}(\xi,\eta)$ by

$$\widetilde{M}_n^{(1)}(\xi,\eta)=\frac{\alpha}{(2\pi i)^2}\int_{\mathcal{C}_1+\overline{\mathcal{C}}_1}d\zeta\int_{\mathcal{D}_1+\overline{\mathcal{D}}_1}d\omega\,\frac{a+z_c}{(a+z_c+\gamma\omega n^{-1/3})(\omega-\zeta)}\times e^{F_\xi(\zeta)-F_\eta(\omega)}. \tag{4.80}$$

Set $\delta_n=a(n)/n^{1/10}$. By assumption $\delta_n\to 0$ as $n\to\infty$. If $|\zeta|\le n^{1/15}$, it follows from (4.71) and (4.78) that $F_\xi(\zeta)=-\zeta^3/3+\xi\zeta+r_n(\zeta)$, where $|r_n(\zeta)|\le C\delta_n^{2/3}$. Also

$$\alpha\left|\frac{a+z_c}{(a+z_c+\gamma\omega n^{-1/3})}-1\right|\le C/a^2, \tag{4.81}$$

if $\omega\in\mathcal{D}_1+\overline{\mathcal{D}}_1$, and thus we can approximate $\widetilde{M}_n^{(1)}(\xi,\eta)$ with

$$\frac{\alpha}{(2\pi i)^2}\int_{\mathcal{C}_1+\overline{\mathcal{C}}_1}d\zeta\int_{\mathcal{D}_1+\overline{\mathcal{D}}_1}d\omega\,e^{-\zeta^3/3+\xi\zeta+\omega/3-\eta\omega}\frac{1}{\omega-\zeta}. \tag{4.82}$$

Note that, if $|\zeta|\ge n^{1/15}$, then $\xi|/|\zeta|^2\le Ca^{4/3}/n^{2/15}\le C\delta_n^{4/3}$ and thus, with a negligible error, we can replace the expression in (4.82) by $\alpha K_{\mathrm{Ai}}(\xi,\eta)$. This completes the proof of the claim and the theorem. □

**5. Gibbs measure.** In this section, we continue our study of the asymptotics of domino tilings with the study of the local Gibbs measure. We denote the asymptotic coordinates by $\xi=(\xi_1,\xi_2)$. That is, for a vertex inside the Aztec diamond denoted by $x=(x_1,x_2)$, we have $x/(2n)\to\xi$. For the remaining calculations of this paper, we use the same saddle point function. This saddle point function is an extension of (4.6) because we now keep track of the asymptotic coordinates. Define

$$g(z;\xi):=g(z;\xi_1,\xi_2):=\xi_2\log(a+z)+(1-\xi_2)\log(az-1)-\xi_1\log z. \tag{5.1}$$

Recall that $\mathcal{D}$ denotes the unfrozen region and is given by the area bounded by the ellipse

$$\frac{(v-u)^2}{1-p}+\frac{(u+v-1)^2}{p}=1, \tag{5.2}$$

where $p=1/(1+a^2)$.

LEMMA 5.1. *The equation $g'(z;\xi_1,\xi_2)=0$ has a unique solution $z=z_\xi$ in $\mathbb{H}$ if and only if $\xi\in\mathcal{D}$.*

PROOF. We expand out the equation $g'(z;\xi_1,\xi_2)=0$. We find that this is equal to

$$-\frac{\xi_1}{z}+\frac{a(1-\xi_2)}{az-1}+\frac{\xi_2}{a+z}=0. \tag{5.3}$$

We solve the above equation with respect to $z$ and the solutions are given by

$$\begin{aligned}(5.4)\qquad &\big(a^2\xi_1 - \xi_1 + \xi_2 + a^2\xi_2 - a^2 \\ &\pm \sqrt{-4a^2(1-\xi_1)\xi_1 + \big(\xi_2 - \xi_1 + a^2(\xi_2+\xi_1-1)\big)^2}\big)/\big(2a(1-\xi_1)\big).\end{aligned}$$

The expression under the square root term in the above equation is given by

$$\begin{aligned}(5.5)\qquad &-4a^2(1-\xi_1)\xi_1 + \big(\xi_2 - \xi_1 + a^2(\xi_2+\xi_1-1)\big)^2 \\ &= \left(\frac{(\xi_1-\xi_2)^2}{a^2} + (\xi_2+\xi_1-1)^2\right)a^2\big(1+a^2\big) - a^2,\end{aligned}$$

which is less than zero if and only if $\xi_1, \xi_2 \in \mathcal{D}$. Therefore, we set

$$\begin{aligned}(5.6)\qquad z_\xi = &\big(a^2\xi_1 - \xi_1 + \xi_2 + a^2\xi_2 - a^2 \\ &+ i\sqrt{4a^2(1-\xi_1)\xi_1 - \big(\xi_2 - \xi_1 + a^2(\xi_2+\xi_1-1)\big)^2}\big) \\ &/\big(2a(1-\xi_1)\big).\end{aligned}$$

□

We now describe the contours of steepest ascent and descent of $g$. In Lemma 5.1, we analyzed the saddle points of $g$. The two nonreal saddle points of $g$ are simple (and are conjugate pairs) and as $g$ is analytic in the upper half plane, the paths of steepest ascent and descent are the level lines of $\operatorname{Im} g$. These paths can cross the real line at $-a, 0, 1/a$. We now describe these paths.

The paths of steepest descent and ascent of the saddle point function are determined in the upper half plane since the lower half plane is a reflection. From the saddle point, there are two paths of steepest ascent, one which goes to $\infty$ while the other ends at 0. From the saddle point, there are two paths of steepest descent, one which ends at $1/a$ and another ending at $-a$. See Figure 9 for an example of the contours of steepest descent and ascent.

We now prove Theorem 2.9.

PROOF OF THEOREM 2.9. Below, we will neglect the integer part in the expressions since they are unimportant. We will only consider the case $x_1 < y_1 + 1$ which means that $K^{-1}(x, y) = f_1(x, y)$ for $x \in \mathtt{W}$ and $b \in \mathtt{B}$. This is due to the following: for $x_1 \geq y_1 + 1$,

$$\begin{aligned}(5.7)\qquad &K^{-1}(x, y) \\ &= f_1(x, y) - f_2(x, y) \\ &= \frac{(-1)^{(x_1+x_2+y_1+y_2)/4}}{(2\pi i)^2} \\ &\quad \times \int_{\gamma_1}\int_{\gamma_2} dw\, dz\, \frac{(a+z)^{x_2/2}(az-1)^{(2n-x_2)/2}w^{(y_1)/2}}{z^{(x_1+1)/2}(w-z)(a+w)^{(y_2+1)/2}(aw-1)^{(2n+1-y_2)/2}},\end{aligned}$$

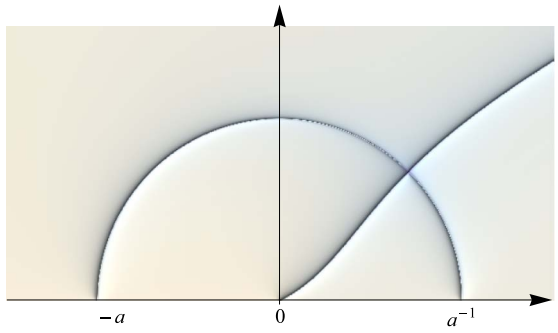


FIG. 9. *A relief plot of* $\log|\operatorname{Im}(g(z;\xi) - g(z_\xi;\xi))|$ *with* $a = 1$, $z_\xi = e^{i\pi/4}$ *and* $\xi = (1/2, \frac{1}{4}(2+\sqrt{2}))$. *The relief plot captures where* $\operatorname{Im} g(z;\xi)$ *is constant and the logarithm is for visual purposes—it sharpens the relief plot. The contour of steepest descent starts at the origin and ends at infinity (goes to the right). The steepest ascent contour starts at* $a^{-1}$ *and ends at* $-a$. *The plot is symmetric in the lower half-plane.*

where $\gamma_2$ is a positively oriented closed contour containing $-a$ and 0 but not $1/a$, and $\gamma_1$ is a positively oriented closed contour containing $\gamma_2$ but not $1/a$. The above formula is found by first moving the contour $\mathcal{E}_2$ in the definition of $f_1(x, y)$ to the contour $\gamma_2$, followed by moving the $\mathcal{E}_1$ through $\gamma_2$ to the contour $\gamma_1$; see Figure 8. This picks up a single integral contribution from $z = w$ (which is negative) with contour of integration around $\gamma_1$. This single integral contribution is equal to $f_2(x, y)$, which is seen by deforming the contour through infinity, which cancels with the term $-f_2(x, y)$ obtained from the split definition of $K^{-1}(x, y)$ for $x_1 \geq y_1 + 1$. Since the double contour integral formula in equation (5.7) is similar to the double contour integral formula in $f_1(x, y)$, the computation of $K^{-1}(x, y)$ for $x_1 > y_1 + 1$ is similar to the computation of $K^{-1}(x, y)$ for $x_1 < y_1 + 1$.

We have $(x_1, x_2) = ([2\xi_1 n] + 2\alpha_1 + 1, [2\xi_2 n] + 2\alpha_2)$ and $(y_1, y_2) = ([2\xi_1 n] + 2\beta_1, [2\xi_2 n] + 2\beta_2 + 1)$ so that $(x_1/(2n), x_2/(2n)) \to (\xi_1, \xi_2) \in [0, 1]^2$ as $n$ tends to infinity. We also have

$$(-1)^{(x_1+x_2+y_1+y_2)/4} = (-1)^{(x_1+x_2-y_1-y_2+2)/4} = i(-1)^{(x_1+x_2-y_1-y_2)/4} \tag{5.8}$$

which follows from the fact that if $y_1 + y_2 \bmod 4 = 2\varepsilon + 1$, then $2 - y_1 + y_2 \bmod 4 = 2\varepsilon + 1$ for $\varepsilon \in \{0, 1\}$. Since

$$(-1)^{(x_1+x_2+y_1+y_2)/4} = i(-1)^{(\alpha_1+\alpha_2-\beta_1-\beta_2)/2}, \tag{5.9}$$

we find that

$$\begin{aligned} &f_1\big((x_1, x_2), (y_1, y_2)\big) \\ &\quad = \frac{i(-1)^{(\alpha_1+\alpha_2-\beta_1-\beta_2)/2}}{(2\pi i)^2} \\ &\qquad \times \int_{\mathcal{E}_2}\int_{\mathcal{E}_1} dz\, dw\, \frac{e^{n(g(z;\xi)-g(w;\xi))}}{w - z} \frac{w^{\beta_1}(a+z)^{\alpha_2}(az-1)^{-\alpha_2}}{z^{\alpha_1+1}(a+w)^{\beta_2+1}(aw-1)^{-\beta_2}}, \end{aligned} \tag{5.10}$$

where $g$ is given in (5.1).

By a computation, we have that $|z_\xi| = r_1$ and

$$\left|\frac{a+z_\xi}{az_\xi - 1}\right| = r_2, \tag{5.11}$$

where $r_1$ and $r_2$ are defined in (2.34).

From Lemma 5.1, we have that for $(\xi_1, \xi_2) \in \mathcal{D}_c$, then $z_\xi \in \mathbb{H}$. By knowing the contours of steepest ascent and descent for $g$ which are given above, we deform the contours $\mathcal{E}_1$ and $\mathcal{E}_2$ accordingly which is the same contour deformation as given in Section 4 of [22]. Explicitly, we move the contour $\mathcal{E}_2$ to go through $\bar{z}_\xi$ and $z_\xi$ passing through the origin and going to infinity. We move $\mathcal{E}_1$ to pass through $z_\xi$ and $\bar{z}_\xi$ which passes either side of the origin of the $x$ axis at $-a$ and $1/a$. Since the contours must cross under this deformation, we pick up an additional single integral from the contribution at $z = w$ along the line $z_\xi$ to $\bar{z}_\xi$. The double contour integral, whose contours of integration are as given above, is $O(n^{-1/2})$; see [37], for example. Note that due to our formulas and orientations of the contours, the additional single integral term comes with a minus sign (due to our formulas). We find that $f_1(x, y)$ is given by

$$\begin{aligned} &-\frac{i(-1)^{(\alpha_1+\alpha_2-\beta_1-\beta_2)/2}}{2\pi i}\int_{\bar{z}_\xi}^{z_\xi} z^{\beta_1-\alpha_1-1}\frac{1}{a+z}\left(\frac{a+z}{az-1}\right)^{\alpha_2-\beta_2} dz \\ &\quad + O\big(n^{-1/2}\big). \end{aligned} \tag{5.12}$$

We make the change of variables $w = t(z) = (a+z)/(az-1)$. With this change of variables $t(w) = z$ and $dz = -(1+a^2)/(aw-1)^2\,dw$. We obtain

$$\begin{aligned} f_1(x, y) &= -\frac{i(-1)^{(\alpha_1+\alpha_2-\beta_1-\beta_2)/2}}{2\pi i} \\ &\quad \times \int_{t(\bar{z}_\xi)}^{t(z_\xi)} t(w)^{\beta_1-\alpha_1-1}\frac{w^{\alpha_2-\beta_2}}{a+((a+w)/(aw-1))}\frac{(-(1+a^2))}{(aw-1)^2}\,dw \\ &\quad + O\big(n^{-1/2}\big) \\ &= \frac{i(-1)^{(\alpha_1+\alpha_2-\beta_1-\beta_2)/2}}{2\pi i}\int_{t(\bar{z}_\xi)}^{t(z_\xi)} t(w)^{\beta_1-\alpha_1-1}\frac{w^{\alpha_2-\beta_2-1}}{aw-1}\,dw \\ &\quad + O\big(n^{-1/2}\big). \end{aligned} \tag{5.13}$$

We have that $|a+w|^2 \le r_1^2|aw-1|^2$ for $w = r_2 e^{i\theta}$ if and only if

$$\begin{aligned} &a^2 + r_2^2\cos^2\theta + 2ar_2\cos\theta + r_2^2\sin^2\theta \\ &\qquad \le r_1^2\big(a^2r_2^2\cos^2\theta - 2ar_2\cos\theta + 1 + a^2r_2^2\sin^2\theta\big) \end{aligned} \tag{5.14}$$

which means that

$$\cos\theta \le \frac{a^2(r_1^2r_2^2-1)+r_1^2-r_2^2}{2r_2a(1+r_1^2)} = \frac{\xi_2-\xi_1+a^2(\xi_1+\xi_2-1)}{2a\sqrt{\xi_1(1-\xi_1)}}. \tag{5.15}$$

The above equation holds with equality if $\theta=\theta_\xi$ where $\theta_\xi=\arg z_\xi$ since

$$\operatorname{Re}(z_\xi) = \frac{\xi_2-\xi_1+a^2(\xi_1+\xi_2-1)}{2a(1-\xi_1)} \tag{5.16}$$

and $|z_\xi| = \sqrt{\xi_1/(1-\xi_1)}$.

Using the residue formula, we write

$$\begin{aligned}\lim_{n\to\infty} f_1(x,y) &= \frac{i(-1)^{(\alpha_1+\alpha_2-\beta_1-\beta_2)/2}}{(2\pi i)^2}\\ &\quad\times\int_{|w|=r_2}\int_{|z|=r_1}\frac{z^{\beta_1-\alpha_1-1}w^{\alpha_2-\beta_2-1}}{(z-((a+w)/(aw-1)))(aw-1)}\,dz\,dw\\ &= \frac{i(-1)^{(\alpha_1+\alpha_2-\beta_1-\beta_2)/2}}{(2\pi i)^2}\\ &\quad\times\int_{|w|=r_2}\int_{|z|=r_1}\frac{z^{\beta_1-\alpha_1-1}w^{\alpha_2-\beta_2-1}}{azw-z-a-w}\,dz\,dw.\end{aligned} \tag{5.17}$$

Take the change of variables $z\mapsto i/z$ and $w\mapsto -i/w$ which gives

$$\begin{aligned}&\lim_{n\to\infty} f_1(x,y)\\ &\quad= \frac{i}{(2\pi i)^2}\int_{|w|=1/r_2}\int_{|z|=1/r_1}\frac{z^{\alpha_1-\beta_1-1}w^{\beta_2-\alpha_2-1}}{a/(zw)-i/z-a+i/w}\,dz\,dw.\end{aligned} \tag{5.18}$$

The above formula, under the change of variables $z\mapsto zr_1$ and $w\mapsto wr_2$, is equal to

$$\frac{r_1^{-\alpha_1+\beta_1}r_2^{-\beta_2+\alpha_2}}{(2\pi i)^2}\int_{|w|=1}\int_{|z|=1}\frac{z^{\alpha_1-\beta_1-1}w^{\beta_2-\alpha_2-1}}{P(zr_1,wr_2)}\,dz\,dw, \tag{5.19}$$

which is equal to

$$r_1^{\alpha_1+\beta_1}r_2^{-\beta_2+\alpha_2}K_\mu^{-1}\big((2\alpha_1+1,2\alpha_2),(2\beta_1,2\beta_2+1)\big). \tag{5.20}$$

Computing the probability of any cylinder event using the above formula in (2.13) is equivalent to the probability of any cylinder event using (2.32) in (2.13) which means we have verified Theorem 2.9 for $x_1<y_1+1$. As mentioned above, a similar argument holds for $x_1\ge y_1+1$, but uses (5.7) instead. □

**6. Discussion on height fluctuations.** In this article, we have focused on studying domino tilings of the Aztec diamond using the information obtained from the inverse Kasteleyn matrix. Here, we briefly discuss the height function associated to domino tilings of the Aztec diamond and its fluctuations in the scaling limit.

The height function, introduced in [43], is defined on the faces of the Aztec diamond graph as follows: the height change between two adjacent faces is $\pm 3$ if there is a dimer covering the shared edge between the two faces and $\mp 1$ otherwise. As we traverse between two adjacent faces, we choose the sign convention to be $+3$ (or, resp., $-3$) if the left vertex is black (or, resp., white). The definition is consistent around each vertex, that is, the total height change around each vertex is zero. Each dimer covering is in bijection (up to a chosen height level) with the height function; see Figure 1 for an example domino tiling and height function.

Denote $h_n(\mathtt{f})$ to be the height function at a face $\mathtt{f}$ in the Aztec diamond graph. Using either the inverse Kasteleyn matrix or the correlation kernel for the red–blue particles, we can compute the moments of height function at faces $\mathtt{f}_1, \dots, \mathtt{f}_m$ (i.e., $\mathbb{E}[\prod_{i=1}^m h_n(\mathtt{f}_i)]$).

The Gaussian free field $F$ on $\mathbb{H}$, the upper half plane, is a probability measure on the set of generalized functions on $\mathbb{H}$ such that for any compactly supported test functions $\phi_1, \phi_2$, $\langle F, \phi_1 \rangle := \int_{\mathbb{H}} F(z)\phi_1(z)|dz|^2$ is a real Gaussian random variable with mean zero and covariance

$$\mathbb{E}\big[\langle F, \phi_1\rangle \langle F, \phi_2\rangle\big] = \int_{\mathbb{H}^2} \phi_1(z_1)\phi_2(z_2)G(z_1, z_2)|dz_1|^2|dz_2|^2, \tag{6.1}$$

where

$$G(z_1, z_2) = -\frac{1}{2\pi}\log\left|\frac{z_1 - z_2}{z_1 - \bar{z}_2}\right|. \tag{6.2}$$

Let $\widetilde{H}_n(\mathtt{f}/(2n)) = h_n(\mathtt{f}) - h_n^a(\mathtt{f})$ where $h_n^a(\mathtt{f})$ is the average height function at the face $\mathtt{f} = (\mathtt{f}_1, \mathtt{f}_2)$ with $\mathtt{f}/(2n) = (\mathtt{f}_1/(2n), \mathtt{f}_2/(2n))$. For $\xi = (\xi_1, \xi_2) \in \mathcal{D}$, we define the map $\Omega : \mathcal{D} \to \mathbb{H}$ by

$$\begin{aligned}\Omega(\xi) = \big(&a^2\xi_1 - \xi_1 + \xi_2 + a^2\xi_2 - a^2 \\ &+ i\sqrt{4a^2(1-\xi_1)\xi_1 - \big(\xi_2 - \xi_1 + a^2(\xi_2 + \xi_1 - 1)\big)^2}\big)/\big(2a(1-\xi_1)\big),\end{aligned} \tag{6.3}$$

which is obtained in the proof of Lemma 5.1.

We expect that for fixed $0 < a < \infty$ and for $\mathtt{f} \in 2n\mathcal{D}$, $\sqrt{\pi}\,\widetilde{H}_n(\mathtt{f}/(2n))$ converges weakly to the $\Omega$-pullback of the Gaussian free field $F$ on $\mathbb{H}$ in the sense

$$\frac{\sqrt{\pi}}{n^2} \sum_{\substack{\mathtt{f} \in 2n\mathcal{D} \\ \text{faces}}} \phi\big(\mathtt{f}/(2n)\big)\widetilde{H}_n(\mathtt{f}) \overset{\text{weakly}}{\longrightarrow} \int_{\mathbb{H}} \phi\big(\Omega^{-1}(z)\big)J(z)F(z)|dz|^2, \tag{6.4}$$

where $J(z)$ is the Jacobian under the change of variables from $z = \Omega(\xi)$ to $\xi$, and the sum is over faces $\mathtt{f}$ in $2n\mathcal{D}$.

We will not prove this but will mention the possible steps that one would need to formulate a proof which is based on [3] where the authors give a complete proof

for the height fluctuations of a certain lozenge tiling model under the pullback of a certain map. First, one would require the following technical estimates based on [3], Section 6:

(1) Compute $K^{-1}(x, y)$ both when $x$ and $y$ are in the bulk and are asymptotically distant where $x$ is in the bulk if $\inf_{\xi \in \partial \mathcal{D}} |x - 2n\xi|_1 > n^{2/3}$, and $x$ and $y$ are asymptotically distant if $|x - y|_1 > n^{1/2+\delta}$ for all $\delta > 0$.

(2) Bound $K^{-1}(x, y)$ both when $x$ and $y$ are asymptotically close, where $x$ and $y$ are asymptotically close if $|x - y|_1 \leq n^{1/2+\delta}$.

(3) Bound $K^{-1}(x, y)$ when either $x$ or $y$, or both, are close to the edge, where $x$ is close to the edge if $n^{1/3} < \inf_{\xi \in \partial \mathcal{D}} |x - 2n\xi|_1 \leq n^{2/3}$, and $x$ is either in the unfrozen or frozen regions.

(4) Bound $K^{-1}(x, y)$ when either $x$ or $y$, or both, are at the edge, where $x$ is at the edge if $\inf_{\xi \in \partial \mathcal{D}} |x - 2n\xi|_1 \leq n^{1/3}$, and $x$ is either in the unfrozen or unfrozen regions.

(5) Bound $K^{-1}(x, y)$ when either $x$ or $y$, or both, are in the frozen regions.

After these estimates are found, one could then use the fact that moments of the height function can be expressed in terms of the inverse Kasteleyn matrix [6, 12, 28–30]. With the above bounds, one could hopefully show that the moment formula for the height function tends to the moments of a Gaussian random variable with variance given by (6.2) for asymptotically distant points in the bulk. After this, one would need an analogous result to [3], Theorem 1.2, which shows that the variance of the height function in the unfrozen region is order $\log n$. Using a result of this form combined with the convergence of moments, one could then conclude the proof as in [3], Section 5.5. See also [39].

Other approaches for proving fluctuations of the height function arising from tiling models have been considered in [14], where the author uses a linear statistic to bypass the rather technical estimates arising from the frozen–unfrozen boundaries and [13], where the author considers the characteristic function of the height function using the Cauchy–Riemann operators. The proofs of the results of [28, 29] do not apply to domino tilings on the Aztec diamond due to the domino tilings studied there had the so-called *Temperley boundary conditions*.

**Acknowledgments.** We would like to thank Alexei Borodin, Maurice Duits, Harald Helfgott, Richard Kenyon, Tony Metcalfe, Jim Propp and David Wilson for enlightening conversations. We would like to thank MSRI (Berkeley) where part of this work was carried out and the Knut and Alice Wallenberg foundation for financial support. We are also very grateful for the anonymous referees whose comments helped in dramatically improving this paper.

## REFERENCES

[1] ANDERSON, G. W., GUIONNET, A. and ZEITOUNI, O. (2010). *An Introduction to Random Matrices*. *Cambridge Studies in Advanced Mathematics* **118**. Cambridge Univ. Press, Cambridge. MR2760897

[2] BORODIN, A. (2002). Duality of orthogonal polynomials on a finite set. *J. Stat. Phys.* **109** 1109–1120. MR1938288
[3] BORODIN, A. and FERRARI, P. L. (2014). Anisotropic growth of random surfaces in $2+1$ dimensions. *Comm. Math. Phys.* **325** 603–684. MR3148098
[4] BORODIN, A., GORIN, V. and RAINS, E. M. (2010). $q$-distributions on boxed plane partitions. *Selecta Math. (N.S.)* **16** 731–789. MR2734330
[5] BORODIN, A. and SHLOSMAN, S. (2010). Gibbs ensembles of nonintersecting paths. *Comm. Math. Phys.* **293** 145–170. MR2563801
[6] BOUTILLIER, C. (2007). Pattern densities in non-frozen planar dimer models. *Comm. Math. Phys.* **271** 55–91. MR2283954
[7] BROOMHEAD, N. (2012). Dimer models and Calabi–Yau algebras. *Mem. Amer. Math. Soc.* **215** viii+86. MR2908565
[8] COHN, H., ELKIES, N. and PROPP, J. (1996). Local statistics for random domino tilings of the Aztec diamond. *Duke Math. J.* **85** 117–166. MR1412441
[9] COHN, H., KENYON, R. and PROPP, J. (2001). A variational principle for domino tilings. *J. Amer. Math. Soc.* **14** 297–346 (electronic). MR1815214
[10] COHN, H., LARSEN, M. and PROPP, J. (1998). The shape of a typical boxed plane partition. *New York J. Math.* **4** 137–165 (electronic). MR1641839
[11] DALEY, D. J. and VERE-JONES, D. (2008). *An Introduction to the Theory of Point Processes*: *General Theory and Structure*, 2nd ed. *Probability and Its Applications* (*New York*) **2**. Springer, New York. MR2371524
[12] DE TILIERE, B. (2007). Conformal invariance of isoradial dimer models & the case of triangular quadri-tilings. *Ann. Inst. H. Poincaré Sect. (B)* **43** 729–750.
[13] DUBÉDAT, J. (2011). Dimers and analytic torsion 1. Available at arXiv:1110.2808.
[14] DUITS, M. (2013). Gaussian free field in an interlacing particle system with two jump rates. *Comm. Pure Appl. Math.* **66** 600–643. MR3020314
[15] ELKIES, N., KUPERBERG, G., LARSEN, M. and PROPP, J. (1992). Alternating-sign matrices and domino tilings. I. *J. Algebraic Combin.* **1** 111–132. MR1226347
[16] ELKIES, N., KUPERBERG, G., LARSEN, M. and PROPP, J. (1992). Alternating-sign matrices and domino tilings. II. *J. Algebraic Combin.* **1** 219–234. MR1194076
[17] FLEMING, B. J. and FORRESTER, P. J. (2011). Interlaced particle systems and tilings of the Aztec diamond. *J. Stat. Phys.* **142** 441–459. MR2771040
[18] GOHBERG, I., GOLDBERG, S. and KRUPNIK, N. (2000). *Traces and Determinants of Linear Operators*. *Operator Theory*: *Advances and Applications* **116**. Birkhäuser, Basel. MR1744872
[19] HELFGOTT, H. (2000). Edge effects on local statistics in lattice dimers: A study of the Aztec diamond (finite case). Preprint. Available at arXiv:math/0007136.
[20] JOCKUSCH, W., PROPP, J. and SHOR, P. (1998). Random domino tilings and the Arctic circle theorem. Preprint. Available at arXiv:math/9801068.
[21] JOHANSSON, K. (2002). Non-intersecting paths, random tilings and random matrices. *Probab. Theory Related Fields* **123** 225–280. MR1900323
[22] JOHANSSON, K. (2005). The arctic circle boundary and the Airy process. *Ann. Probab.* **33** 1–30. MR2118857
[23] JOHANSSON, K. (2006). Random matrices and determinantal processes. In *Mathematical Statistical Physics* 1–55. Elsevier, Amsterdam. MR2581882
[24] JOHANSSON, K. and NORDENSTAM, E. (2006). Eigenvalues of GUE minors. *Electron. J. Probab.* **11** 1342–1371. MR2268547
[25] KASTELEYN, P. W. (1961). The statistics of dimers on a lattice: I. The number of dimer arrangements on a quadratic lattice. *Physica* **27** 1209–1225.
[26] KASTELEYN, P. W. (1963). Dimer statistics and phase transitions. *J. Math. Phys.* **4** 287–293. MR0153427

[27] KENYON, R. (1997). Local statistics of lattice dimers. *Ann. Inst. Henri Poincaré Probab. Stat.* **33** 591–618. MR1473567

[28] KENYON, R. (2000). Conformal invariance of domino tiling. *Ann. Probab.* **28** 759–795. MR1782431

[29] KENYON, R. (2001). Dominos and the Gaussian free field. *Ann. Probab.* **29** 1128–1137. MR1872739

[30] KENYON, R. (2008). Height fluctuations in the honeycomb dimer model. *Comm. Math. Phys.* **281** 675–709. MR2415464

[31] KENYON, R. (2009). Lectures on dimers. In *Statistical Mechanics. IAS/Park City Math. Ser.* **16** 191–230. Amer. Math. Soc., Providence, RI. MR2523460

[32] KENYON, R. and OKOUNKOV, A. (2007). Limit shapes and the complex Burgers equation. *Acta Math.* **199** 263–302. MR2358053

[33] KENYON, R., OKOUNKOV, A. and SHEFFIELD, S. (2006). Dimers and amoebae. *Ann. of Math.* (2) **163** 1019–1056. MR2215138

[34] LEVITOV, L. S. (1989). The rvb model as the problem of the surface of a quantum crystal. *JETP Lett.* **50** 469–472.

[35] LEVITOV, L. S. (1990). Equivalence of the dimer resonating-valence-bond problem to the quantum roughening problem. *Phys. Rev. Lett.* **64** 92–94. MR1031942

[36] LUBY, M., RANDALL, D. and SINCLAIR, A. (2001). Markov chain algorithms for planar lattice structures. *SIAM J. Comput.* **31** 167–192. MR1857394

[37] OKOUNKOV, A. and RESHETIKHIN, N. (2003). Correlation function of Schur process with application to local geometry of a random 3-dimensional Young diagram. *J. Amer. Math. Soc.* **16** 581–603 (electronic). MR1969205

[38] PETROV, L. (2012). Asymptotics of random lozenge tilings via Gelfand–Tsetlin schemes. Available at arXiv:1202.3901.

[39] PETROV, L. (2012). Asymptotics of uniformly random lozenge tilings of polygons. Gaussian free field. Available at arXiv:1206.5123.

[40] ROMIK, D. (2012). Arctic circles, domino tilings and square Young tableaux. *Ann. Probab.* **40** 611–647. MR2952086

[41] SOSHNIKOV, A. (2000). Determinantal random point fields. *Uspekhi Mat. Nauk* **55** 107–160. MR1799012

[42] TEMPERLEY, H. N. V. and FISHER, M. E. (1961). Dimer problem in statistical mechanics—an exact result. *Philos. Mag.* (8) **6** 1061–1063. MR0136398

[43] THURSTON, W. P. (1990). Conway's tiling groups. *Amer. Math. Monthly* **97** 757–773. MR1072815

S. CHHITA
INSTITUTE FOR APPLIED MATHEMATICS
UNIVERSITY OF BONN
ENDENICHER ALLEE 60
D-53115 BONN
GERMANY
E-MAIL: schhita@iam.uni-bonn.de
chhita@kth.se

K. JOHANSSON
DEPARTMENT OF MATHEMATICS
ROYAL INSTITUTE OF TECHNOLOGY (KTH)
SE-100 44 STOCKHOLM
SWEDEN
E-MAIL: kurtj@kth.se

B. YOUNG
DEPARTMENT OF MATHEMATICS
UNIVERSITY OF OREGON
EUGENE, OREGON 97403
USA
E-MAIL: bjy@uoregon.edu